



**NAVAL
POSTGRADUATE
SCHOOL**

MONTEREY, CALIFORNIA

THESIS

**EXTRACTING HIDDEN TRAILS AND ROADS UNDER
CANOPY USING LIDAR**

by

Apostolos Karatolios
Prokopios Krougios

December 2008

Thesis Advisor:
Thesis Co-Advisor:

R.C. Olsen
David C. Jenn

Approved for public release; distribution is unlimited

THIS PAGE INTENTIONALLY LEFT BLANK

REPORT DOCUMENTATION PAGE			<i>Form Approved OMB No.</i>
Public reporting burden for this collection of information is estimated to average 1 hour per response, including the time for reviewing instruction, searching existing data sources, gathering and maintaining the data needed, and completing and reviewing the collection of information. Send comments regarding this burden estimate or any other aspect of this collection of information, including suggestions for reducing this burden, to Washington headquarters Services, Directorate for Information Operations and Reports, 1215 Jefferson Davis Highway, Suite 1204, Arlington, VA 22202-4302, and to the Office of Management and Budget, Paperwork Reduction Project (0704-0188) Washington DC 20503.			
1. AGENCY USE ONLY (Leave blank)	2. REPORT DATE December 2008	3. REPORT TYPE AND DATES COVERED Master's Thesis	
4. TITLE AND SUBTITLE Extracting Hidden Trails and Roads Under Canopy Using LIDAR		5. FUNDING NUMBERS	
6. AUTHOR(S) Apostolos Karatolios and Prokopios Krougios		8. PERFORMING ORGANIZATION REPORT NUMBER	
7. PERFORMING ORGANIZATION NAME(S) AND ADDRESS(ES) Naval Postgraduate School Monterey, CA 93943-5000		10. SPONSORING/MONITORING AGENCY REPORT NUMBER	
9. SPONSORING /MONITORING AGENCY NAME(S) AND ADDRESS(ES) N/A		11. SUPPLEMENTARY NOTES The views expressed in this thesis are those of the author and do not reflect the official policy or position of the Department of Defense or the U.S. Government.	
12a. DISTRIBUTION / AVAILABILITY STATEMENT Approved for public release; distribution is unlimited		12b. DISTRIBUTION CODE	
13. ABSTRACT (maximum 200 words) The field of Remote Sensing has been greatly benefited by the development of LIDAR. The extraction of bare earth under tree canopies and especially the identification of hidden trails are important tools for military and civilian operations in dense forests. LIDAR data from Sequoia National Park in California (2008) and Fort Belvoir Military Base in Virginia (2007) were two areas that were selected for analysis. Quick Terrain Modeler software was used in order to recognize hidden trails. The entire procedure was followed by ground truth verifications in Sequoia National Park and all the necessary preparations for the analysis of Fort Belvoir data were studied. The ground truth results in Sequoia were promising and the analysis of Fort Belvoir data was encouraging for further development of the system. Trails with a width less than 2 m were easily recognized in Fort Belvoir during the analysis of the data, which affirmed the high accuracy of the sensor. In the Sequoia area, only paved trails with a width less than 1.5 m were identified.			
14. SUBJECT TERMS LIDAR, Ladar, Laser Radar, Foliage Penetration, FOPEN, Poke-Through, Terrain Analysis, Trails, Sequoia National Park, Fort Belvoir Virginia, Hidden Trails, Quick Terrain Modeler, LIDAR Accuracy, LIDAR Error		15. NUMBER OF PAGES 115	
		16. PRICE CODE	
17. SECURITY CLASSIFICATION OF REPORT Unclassified	18. SECURITY CLASSIFICATION OF THIS PAGE Unclassified	19. SECURITY CLASSIFICATION OF ABSTRACT Unclassified	20. LIMITATION OF ABSTRACT UU

NSN 7540-01-280-5500

Standard Form 298 (Rev. 2-89)
Prescribed by ANSI Std. Z39-18

THIS PAGE INTENTIONALLY LEFT BLANK

Approved for public release; distribution is unlimited

**EXTRACTING HIDDEN TRAILS AND ROADS
UNDER CANOPY USING LIDAR**

Apostolos Karatolios
Captain, Greek Air Force
B.S., Hellenic Air Force Academy, 1994

Submitted in partial fulfillment of the
requirements for the degree of

MASTER OF SCIENCE IN APPLIED PHYSICS

Prokopios Krougios
Lieutenant Junior Grade, Greek Navy
B.S., Hellenic Naval Academy, 2000

Submitted in partial fulfillment of the
requirements for the degree of

MASTER OF SCIENCE IN APPLIED PHYSICS

and

MASTER OF SCIENCE IN ELECTRONIC WARFARE SYSTEMS ENGINEERING

from the

**NAVAL POSTGRADUATE SCHOOL
December 2008**

Authors: Apostolos Karatolios

Prokopios Krougios

Approved by: R.C. Olsen
Thesis Advisor

David C. Jenn
Thesis Co-Advisor

James Luscombe
Chairman, Department of Physics

Dan C. Boger
Chairman, Department of Information Sciences

THIS PAGE INTENTIONALLY LEFT BLANK

ABSTRACT

The field of Remote Sensing has been greatly benefited by the development of LIDAR. The extraction of bare earth under tree canopies and especially the identification of hidden trails are important tools for military and civilian operations in dense forests. LIDAR data from Sequoia National Park in California (2008) and Fort Belvoir Military Base in Virginia (2007) were two areas that were selected for analysis. Quick Terrain Modeler software was used in order to recognize hidden trails. The entire procedure was followed by ground truth verifications in Sequoia National Park and all the necessary preparations for the analysis of Fort Belvoir data were studied. The ground truth results in Sequoia were promising and the analysis of Fort Belvoir data was encouraging for further development of the system. Trails with a width less than 2 m were easily recognized in Fort Belvoir during the analysis of the data, which affirmed the high accuracy of the sensor. In the Sequoia area, only paved trails with a width less than 1.5 m were identified.

THIS PAGE INTENTIONALLY LEFT BLANK

TABLE OF CONTENTS

I.	INTRODUCTION.....	1
A.	GENERAL.....	1
B.	OBJECTIVE	1
C.	RESEARCH STRUCTURE.....	1
II.	BACKGROUND	3
A.	LIDAR.....	3
B.	LIDAR EVOLUTION	7
C.	PROCESSING FORESTRY LIDAR DATA.....	11
1.	Discrete Return LIDAR	11
2.	Waveform LIDAR Systems and Analysis.....	15
3.	LIDAR Data Extracted Information.....	21
4.	Discrete Returns vs. Waveform Data.....	23
D.	LIDAR BENEFITS.....	24
E.	WHY LIDAR?.....	27
F.	LIDAR ACCURACY AND ERRORS	28
1.	Accuracy	28
2.	Errors.....	30
a.	<i> Laser Rangefinder Error</i>	<i> 30</i>
b.	<i> GPS Positioning Error.....</i>	<i> 31</i>
c.	<i> IMU Orientation Error</i>	<i> 32</i>
d.	<i> Filtering Processing Error.....</i>	<i> 32</i>
e.	<i> Errors in LIDAR Ground Elevation and Wetland Vegetation Height Estimates</i>	<i> 33</i>
G.	LIDAR APPLICATIONS	35
1.	Civilian Applications	35
a.	<i> Geology-Seismology.....</i>	<i> 35</i>
b.	<i> Forestry.....</i>	<i> 35</i>
c.	<i> Sea Ice</i>	<i> 36</i>
d.	<i> Mapping.....</i>	<i> 37</i>
e.	<i> Oil and Gas Exploration</i>	<i> 38</i>
f.	<i> Corridor Mapping</i>	<i> 38</i>
g.	<i> Flood Plain Mapping</i>	<i> 39</i>
2.	Military Applications.....	39
a.	<i> Bathymetry</i>	<i> 40</i>
b.	<i> Rapid Airborne Mine Clearance System (RAMICS).....</i>	<i> 40</i>
c.	<i> Super-Sensitive Imaging Systems.....</i>	<i> 41</i>
d.	<i> LIDAR for Missile Interceptors.....</i>	<i> 42</i>
III.	PROJECT DESCRIPTION	43
A.	OVERVIEW	43
B.	LIDAR DATA LOCATIONS	44
1.	Fort Belvoir.....	45

2.	Sequoia National Park	49
C.	FIELD EQUIPMENT.....	52
IV.	OBSERVATIONS.....	53
A.	TRAIL AND ROAD CLASSIFICATION	53
B.	RESEARCH METHODOLOGY	57
C.	DATA COLLECTION TOOLS AND PROCEDURES	60
V.	ANALYSIS	65
A.	FORT BELVOIR.....	65
B.	SEQUOIA NATIONAL PARK	68
VI.	SUMMARY AND CONCLUSIONS	73
A.	SUMMARY	73
B.	CONCLUSION	74
	APPENDIX A. FORESTRY DATA PROCESS USING QTM TOOLS	77
A.	BARE EARTH EXTRACTION	77
B.	DISPLAY TOOLS	79
	APPENDIX B. ACCURACY TEMPLATES	83
	LIST OF REFERENCES.....	91
	INITIAL DISTRIBUTION LIST	97

LIST OF FIGURES

Figure 1.	(a) Collection of georectified digital aerial photographs and high-resolution LIDAR data over an area of interest. (b) The instrument uses a green laser and a raster scanning mechanism to acquire LIDAR data while a GPS base station locates the position of the aircraft and receives the collected data (From: www.sanctuariesimon.org and www.soundwaves.usgs.gov/2007/09/meetings2.html).....	4
Figure 2.	LIDAR Acquisition System (From: www.valtus.com)	5
Figure 3.	Differences between waveform and discrete-return LIDAR	7
Figure 4.	Maiman’s ruby laser (From: http://laserstars.org/history/ruby.html)	8
Figure 5.	First measurements of terrain and trees from the NASA Airborne Oceanographic LIDAR (AOL) (From: Krabill et al., 1984).....	9
Figure 6.	Results from the Shuttle Laser Altimeter (From: NASA, 2008)	10
Figure 7.	Profile 1 through forest, buildings, and corn field (From: Hug et al., 2004)...11	11
Figure 8.	Typical airborne commercial discrete return LIDAR scanning system (From: Lewis and Hancock, 2007).	12
Figure 9.	LIDAR misperceived tree heights measurements (From: Lewis and Hancock, 2007).....	13
Figure 10.	Angle effects on tree height measurements (From: Lewis and Hancock, 2007).	13
Figure 11.	Slope effects (From: Lewis and Hancock, 2007).....	14
Figure 12.	LIDAR intensity (From: Kalogirou, 2006).....	14
Figure 13.	Waveform LIDAR Operation (From: Lewis and Hancock, 2007).....	16
Figure 14.	Riegl LiteMapper 5600 data from a Corn Field (see also Figure 7 above) (From: Hug et al., 2004).	16
Figure 15.	3-D point cloud of the study area. The color shows the index of the corresponding scatterer. (a) Points presenting only one echo pulse are in green. (b) Points presenting two echoes and more are in grey and blue (From: Ducic et al., 2006).....	17
Figure 16.	(a) Amplitude image showing trees, vegetation, access roads and buildings. (b) Pulse width image (From: Ducic et al., 2006).....	18
Figure 17.	SLICER operation (From: Dubayah et al., 1997).....	19
Figure 18.	Steps in converting a raw SLICER waveform to various processing levels. (From: Progress in Lidar Altimeter Remote Sensing of Stand Structure, In Deciduous and Coniferous Forests Using Slicer Data; Michael A. Lefsky, David J. Harding, Geoffery G. Parker ,Warren B. Cohen, Steven A. Acker; Proceedings of the ISPRS Workshop; Mapping Surface Structure And Topography by Airborne and Spaceborne Lasers; November 9-11, 1999; La Jolla, CA; ISPRS WG III/5: Remote Sensing and Vision Theories for Automatic Scene Interpretation; ISPRS WG III/2: Algorithms for Surface Reconstruction; International Archives of Photogrammetry And Remote Sensing; XXXII-3/W14 (http://www.isprs.org/commission3/lajolla/).....	20

Figure 19.	(a) LVIS can be mounted on any aircraft that has a standard aerial camera mount and a window. (b) These sample data show bare-earth topography for an urban and forested region in central Maryland, collected in leaf-on conditions. Above right: Vertical extent of vegetation and buildings in the same region of central Maryland. Blue areas are flat (i.e., roads), and yellow and red areas are tree heights ranging from 25-30 meters.	21
Figure 20.	(a) Histogram of the pulse width of points. (b) Histogram of the amplitude of points. The blue points correspond to one echo and the red ones to multiple echoes. (From: Ducic et al., 2006).....	23
Figure 21.	Echo signals from different target situations. For every target type from left to right: sketch of target and laser beam, discrete return result, full waveform echo signal.	24
Figure 22.	Laser radar beams light up the sky on a winter's night at the LIDAR Research Laboratory in Chatanika, Alaska as part of an international collaborative study of the polar atmosphere. (From: Emison, 2008)	25
Figure 23.	GPS communication with LIDAR system (From: www.forestry.gov.uk)	29
Figure 24.	This figure demonstrates how a single coherent beam of laser light is diffracted into an angular field. An error can occur due to geometric relationships imposed by axial mounting considerations between the camera and the laser field generator	31
Figure 25.	Error in IMU-derived position. The diagram shows the error in the position derived from the stand-alone IMU for one minute	32
Figure 26.	The scan angle must be within 18° of nadir; otherwise, LIDAR footprint can become highly distorted (From: www.cnrhome.uidaho.edu).....	34
Figure 27.	The Seattle Fault between Puget Sound and Seattle.....	35
Figure 28.	Total amounts of stored carbon in black, and annual carbon fluxes in purple. (From: NASA Earth Science Enterprise)	36
Figure 29.	Geikie ice cap (From: Forsberg, R. et al., 2003).....	37
Figure 30.	The photo above shows the 0.1 ft. RMSE accuracy of the 20-mile corridor project T-REX, Denver, CO in 2000.	38
Figure 31.	Corridor picture analyzed and converted to LIDAR data imaging.....	39
Figure 32.	Bathymetric LIDAR waveform (From: Schlagintweit, 1993).....	40
Figure 33.	Rapid Airborne Mine Clearance System (RAMICS) and Airborne Laser Mine Detection System (ALMDS) (From: Global Security Organization, 2008)	41
Figure 34.	(a) Fort Belvoir original QTM image and (b) bare earth extracted image.....	43
Figure 35.	(a) Cropped trail ('target' area) and (b) Cropped 'control' area.....	44
Figure 36.	Fort Belvoir in Virginia (From: Google Map).....	45
Figure 37.	Sequoia National Park in California (From: Google Map).....	45
Figure 38.	Area covered by LIDAR sensor.....	46
Figure 39.	Flight passes.....	46
Figure 40.	The ALTM 3100EA is the solution for engineering and corridor applications to collect higher altitude missions if demanded	47
Figure 41.	(a) top view from Moro Rock, (b) meadow surrounded with pine trees	49
Figure 42.	Selected three areas for trail identification	50

Figure 43.	Area covered by Airborne 1 flight.....	51
Figure 44.	Screen capture of the flight parameters that were used on the captured LIDAR images.....	51
Figure 45.	Trails samples in Sequoia National Park and Fort Belvoir.....	53
Figure 46.	Road nomenclature	55
Figure 47.	Paved trail in Sequoia National Park	56
Figure 48.	Unpaved trail in Sequoia National Park.....	56
Figure 49.	Randomly generated points for both target and control areas.	57
Figure 50.	Point #1 is considered to be inside the range of 50 cm radius cycle, while Point #2 is outside. Point #2 was not characterized as a successful result due to its distance from the reference point.	58
Figure 51.	Red dots represent the points (targets and controls) and the arrows show the direction of the trail. Blue dashed lines are perpendicular to the mean direction axis of the trail and pass from the point. The signs + or – represent the distance that is forward or backward (respectively) of the point and have a positive or negative number.	60
Figure 52.	Rescale model height tool: (a) exaggerated top view showing the depression in Sequoia National Park (b) default values for the depression in that area.....	61
Figure 53.	Creek with a width of two meters width in Fort Belvoir measured by QTM and its corresponding intensity profile.....	62
Figure 54.	The rough fluctuations on the bottom of the “well” along the intensity profile correspond to the <i>asphalt</i> paved trail	63
Figure 55.	The rough fluctuations on the bottom of the “well” along the intensity profile correspond to the <i>wooden</i> paved trail.....	64
Figure 56.	Area 4B and its corresponding height profile below	67
Figure 57.	High resolution of Fort Belvoir Data illustrates the three images	68
Figure 58.	Unpaved trails not identified with LIDAR data.....	69
Figure 59.	The resolution features from (a) Fort Belvoir and (b) Sequoia National Park	70

THIS PAGE INTENTIONALLY LEFT BLANK

LIST OF TABLES

Table 1.	Absolute vertical accuracy.....	27
Table 2.	Absolute horizontal accuracy.....	27
Table 3.	Optech 3100 Specifications (From: Optech, 2008)	48
Table 4.	Field Equipment.....	52
Table 5.	Road classification according to the number of lanes	55
Table 6.	Template, similar to those created from the experiment, used to analyze the results	59
Table 7.	Fort Belvoir Sub-areas size and its corresponding target and control points ..	66
Table 8.	Sequoia Sub-areas size and its corresponding target and control points	70
Table 9.	Total results from Sequoia Measurements.....	71

THIS PAGE INTENTIONALLY LEFT BLANK

ACKNOWLEDGMENTS

Special Thanks to:

Dr. R.C. Olsen, Naval Postgraduate School

Dr D. Jenn, Naval Postgraduate School

Angela Puetz, Naval Postgraduate School

Krista Lee, Naval Postgraduate School

Daria Siciliano, Naval Postgraduate School

Elise Macpherson, Airborne 1 Corporation

Pavlos Kassomenos, University of Ioannina, Greece

Maria and Theofania Karatoliou

Chrysoula and Giannis Krougios

THIS PAGE INTENTIONALLY LEFT BLANK

I. INTRODUCTION

A. GENERAL

The field of Remote Sensing provides an important tool for the definition of the environment in both the civilian and military worlds. One of the most recent forms of remote sensing is **L**ight **D**etection and **R**anging, or LIDAR. Modern LIDAR systems provide the ability to acquire very accurate 3-D surface images of the world, and have a wide variety of applications, including urban and forest topography.

One of the primary problems in remote sensing is to see below the top layer of forest canopies, in order to observe natural and manmade features under the trees. This is very difficult to do with passive optical sensors, or imaging radar. An emerging capability with LIDAR sensors is to see ‘what happens’ below the tops of trees in dense forests. Many human facilities of special interest are hidden in the jungle, making them difficult to locate. LIDAR systems have become important for the identification of any legal or illegal operations under tree canopies. One way to detect them is to recognize any possible trails and roads that indicate any movement of people between areas of interest. The purpose of this thesis is to study the utility of LIDAR for this kind of identification.

B. OBJECTIVE

The overall goal of this thesis is evaluate the utility of LIDAR systems for finding hidden roads and trails under canopy. This thesis will also review the development of LIDAR technology, particularly airborne scanning LIDAR systems. One commercial software package, Quick Terrain Modeler, will be used for processing and extracting ground information.

C. RESEARCH STRUCTURE

The object of the research is to extract trail information in urban and forestry areas from aerial imagery and LIDAR point clouds.

Chapter II presents a review of general LIDAR characteristics as found in published research papers and other sources. This chapter describes LIDAR techniques, development and current capabilities of civilian and military LIDAR. The differences between discrete and waveform LIDAR systems are described to better understand the results and the data accuracy. A reference to LIDAR errors is also added.

For the areas selected, all the LIDAR data and the real images were thoroughly searched and appear in Chapter III. A description of selected areas and field equipment used are also described.

Chapter IV is devoted to trail classification containing some fundamental characteristics from civilian/military aspects of trails. Moreover, statistical methodology used for the evaluated results and several useful tools helpful in obtaining the best analysis and results are contained in this chapter.

Chapter V described the analysis of datasets and the results for the areas. A detailed description of the analysis and all the numerical results concentrated after the measurements are provided. Finally, the summary, conclusions and recommendations given in Chapter VI are based on the experimental results.

II. BACKGROUND

A. LIDAR

Light Detection and Ranging (LIDAR) is a developing technology used in remote sensing to exploit the properties of scattered and reflected light. LIDAR systems make it possible to develop a 3-D depiction of urban and forest structure and can accurately estimate ground elevations, the structure of vegetation and manmade structures under tree canopies. LIDAR makes it possible to create topographic maps, focusing on modeling, mapping and forestry. The unique capabilities of advanced laser systems, combined with the contribution of Inertial Measuring Unit (IMU)) and Global Positioning System (GPS) technologies create an alternative method of precise topographic information. These newer capabilities are advantageous compared to the classical methods of remote sensing and surveying. LIDAR is an active technology that works similarly to radar (which uses radio waves instead of light) by transmitting laser pulses to a target and recording the time it takes for the pulse to return to the sensor's receiver. A much shorter wavelength (near infrared) is used (by comparison to radar), resulting in greater spatial resolution. Light beams from lasers can penetrate the tree canopy through gaps in branches and leaves and be observed reflecting from the ground (Figure 1). This supplies observers with a "see through" capability. Comparable to the sun's rays on a bright day, LIDAR technology maps the ground surface by penetrating the tree canopy.

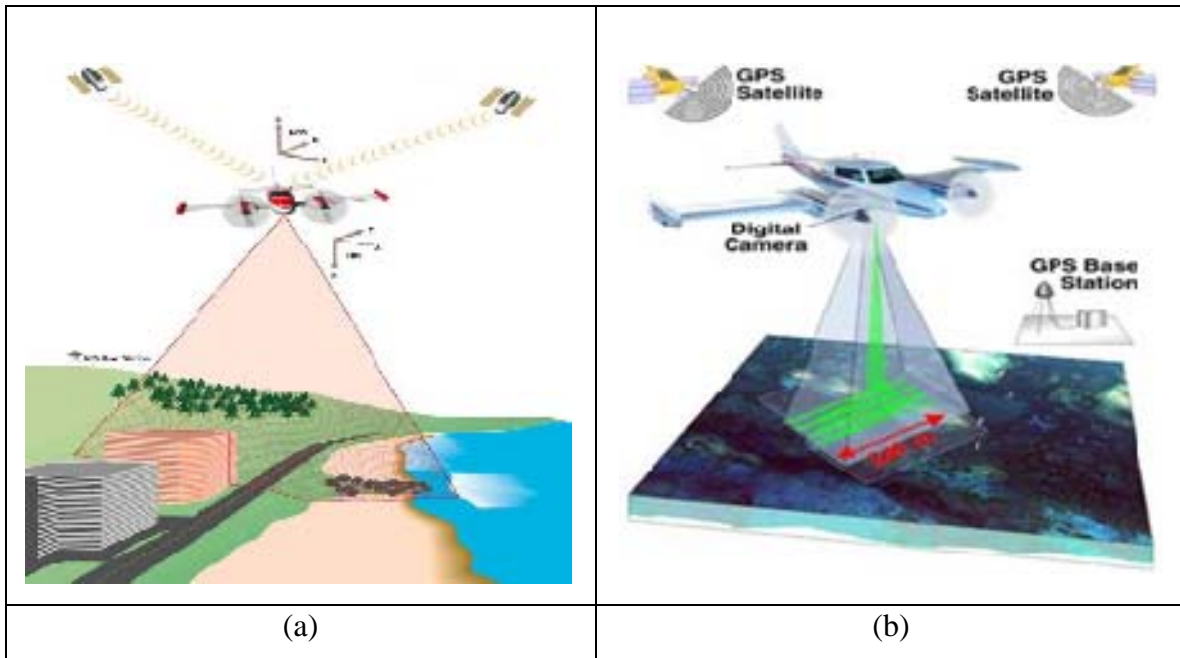


Figure 1. (a) Collection of georectified digital aerial photographs and high-resolution LIDAR data over an area of interest. (b) The instrument uses a green laser and a raster scanning mechanism to acquire LIDAR data while a GPS base station locates the position of the aircraft and receives the collected data (From: www.sanctuariesimon.org and www.soundwaves.usgs.gov/2007/09/meetings2.html)

LIDAR measures the pulse return time to determine surface elevations. LIDAR data, for terrestrial applications, generally have wavelengths ranging from 900-1064 nanometers, due to the vegetation's high level of reflectance (Ensminger, 2007). Visible wavelengths are not preferred because the vegetation absorbance is high and only a small amount of energy would be returned to the sensor. Longer (infrared) wavelengths reduce the effects of atmospheric absorption and scattering.

The LIDAR system is mounted at the bottom of an aircraft and scans the area below the airplane, emitting laser light in a perpendicular direction to the flight path. Parallel flight paths create an overlap of scanning areas and provide a complete image of the target area. In order to determine the orientation of the area and the position of all cloud points, it combines the GPS and the Inertial Navigation System (INS) of the aircraft with the current scan angle of a rotating mirror that emits a laser beam and a laser range finder. The IMU measures the scan angle of the mirror at the moment of each pulse

and records the precise pitch, roll and heading of the aircraft (Figure 2). It is eye-safe and laser scanning occurs day and night, providing that good weather conditions are present (the sky is clear).

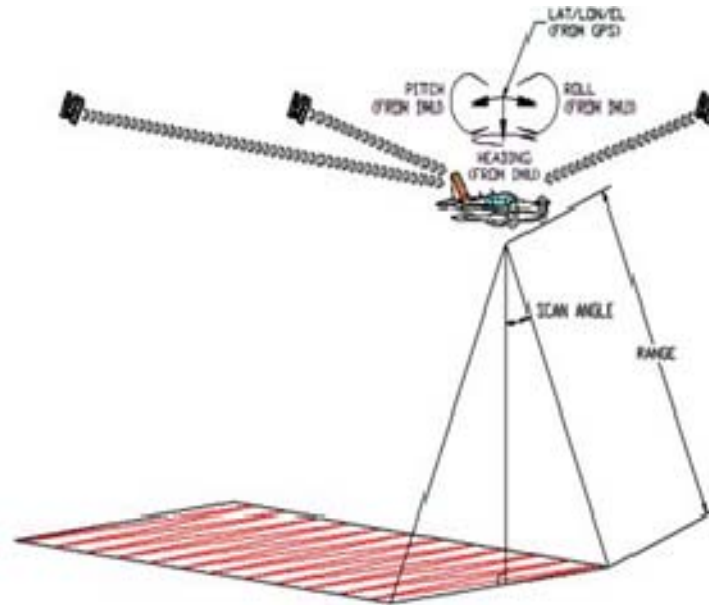


Figure 2. LIDAR Acquisition System (From: www.valtus.com)

Some parameters are taken into consideration during the collection of data. First, the most important aspect is the pulse rate per second of the laser beam that is transmitted from the sensor to the earth's surface. A higher pulse rate gives higher resolution because it increases the probability that the laser beam will penetrate the canopy and hit other objects like branches or the ground. Next, the output power of the LIDAR is considered, because that defines the flight altitude. Higher output power permits researchers to fly at higher altitudes and scan larger areas for a given field of view. Furthermore, the intensity, or power, of the return signal depends on additional factors besides the output power: the small portion of the laser pulse that is interrupted by a surface, the intercepted reflectance on the surface at the wavelength of the laser and the fraction of the illumination that is reflected and travels back toward the sensor (Ducic et al., 2006).

A major application of LIDAR includes mapping, used to image buildings, road construction and other man-made structures. A modern LIDAR system can collect from

10 to 100 thousand 3-D points per second and supplies a resolution 1-40 points per square meter, depending on the flight altitude and airspeed (Mangold, 2008). Various LIDAR companies begun to demonstrate that the integration of LIDAR with multi-spectral imagery (MSI). The combination of LIDAR and MSI allow for the production of bare earth modeling and the classification of the terrain.

The type of data collected from backscattering, distinguishes two broad categories of sensors. One category is the discrete-return LIDAR sensors that measure from one up to seven returns (multiple-return systems). It measures major peaks that represent discrete objects in the path of the laser illumination (Lefsky et al., 2002). A Digital Surface Model (DSM) is generated by the selection of the first echo. The last echoes are the starting point for generating the Digital Terrain Model (DTM). For hard surface reflectors, such as house roofs or roads, these echoes are identical (TopoSys, 2008).

During the last decade, a new generation of airborne laser scanners has appeared, making it feasible to digitize and record the entire backscattered signal of each emitted pulse. It is also possible to identify the type and the material of the target. This advanced technology is called full waveform (FW) LIDAR (Chauve et al., 2007). Figure 3 illustrates conceptual differences between discrete and waveform categories of LIDAR sensors.

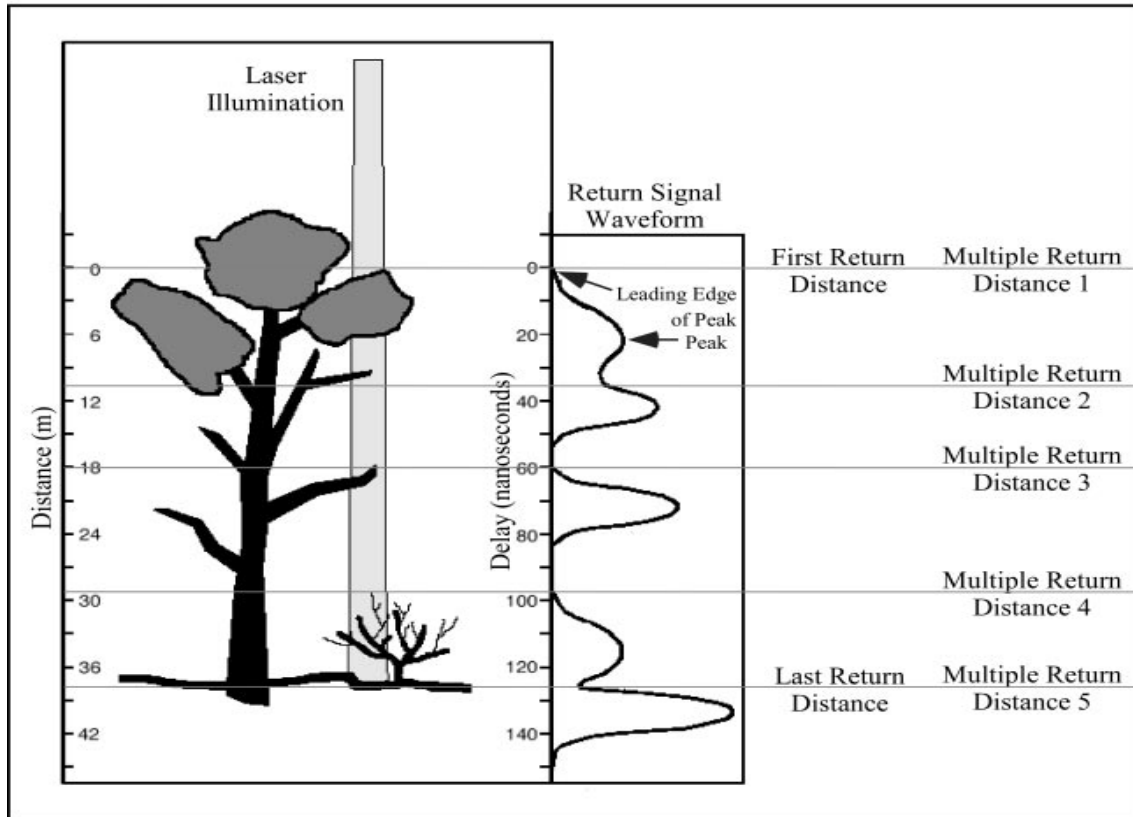


Figure 3. Differences between waveform and discrete-return LIDAR

B. LIDAR EVOLUTION

The invention of the laser was a landmark in the history of LIDAR. Arthur Schawlow and C. H. Townes first developed the theory of the laser, as given in the landmark paper “Infrared and optical masers” (Schawlow and Townes, 1958). Theodore Maiman then demonstrated the first laser on May 16, 1960 at Hughes Research Laboratories. The components of Maiman's solid state (ruby) laser are illustrated below (Figure 4) (Maiman, 1960). Since then, lasers have enormous applications in all sciences and billions of dollars have been invested in the laser industry (Garwin and Lincoln, 2003).

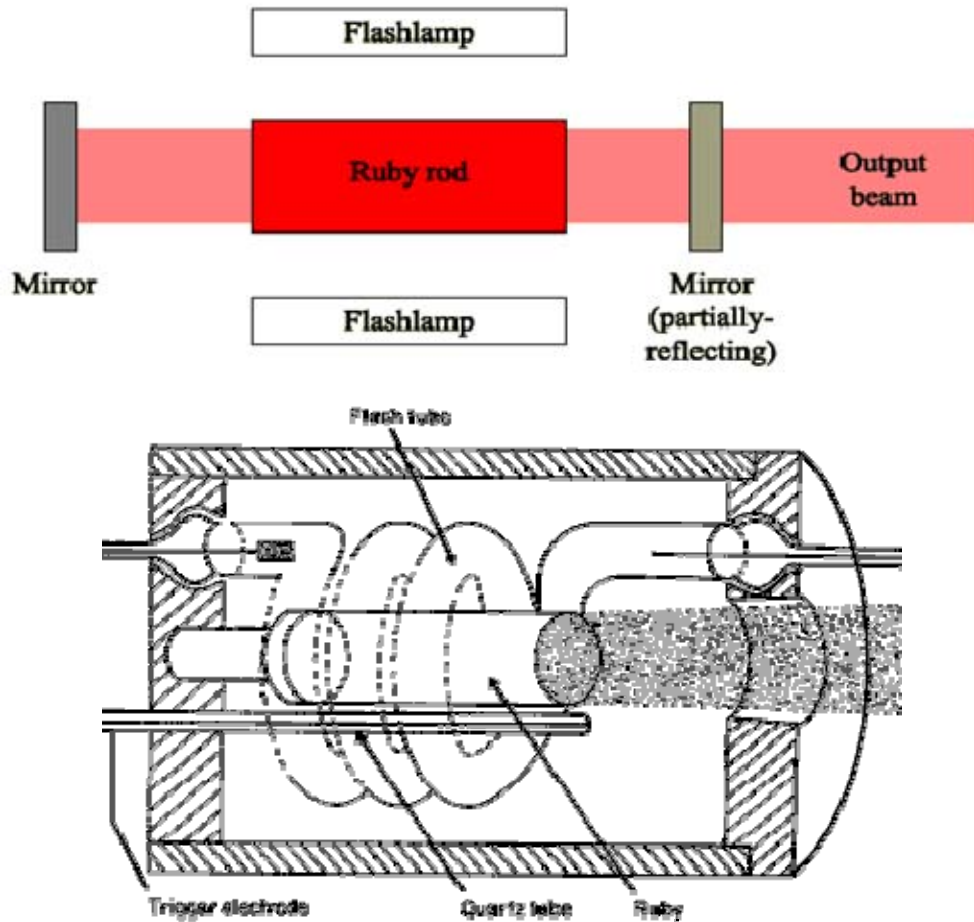


Figure 4. Maiman's ruby laser (From: <http://laserstars.org/history/ruby.html>)

Currently, most LIDAR sensors use neodymium-doped yttrium aluminum garnet (**Nd:YAG**), a glass material working at 1.064 microns (μ) (Geusic et al., 1964).

Solodukhin was the pioneer scientist who developed LIDAR in the Soviet Union in 1977. He first attempted to use lasers to estimate the forest biomass (Solodukhin et al., 1977).

This attempt was followed by studies in North America in the early 1980s. NASA, in the 1970s, developed a measurement technique using LIDAR, and was commercially used since the early 1990s (Bartels, 2007).

The first LIDAR systems measured the altitude of the aircraft to assure the accuracy of the flight pattern. Once airborne, the sensor emits pulses of infrared laser light, which are used to determine ranges to points on the ground. The time difference between the transmit pulse and the receive pulse is a measure of height. Subsequently, Airborne Laser Scanning (ALS) systems emerged. The first terrestrial LIDAR flight apparently was performed in 1979, by the NASA Airborne Oceanographic LIDAR (AOL), a technology designed for bathymetry (Krabill et al., 1984). The first full-waveform (FW) LIDAR system was developed in the 1980s (Figure 5), again for bathymetric purposes (Guenther and Mesick, 1988).

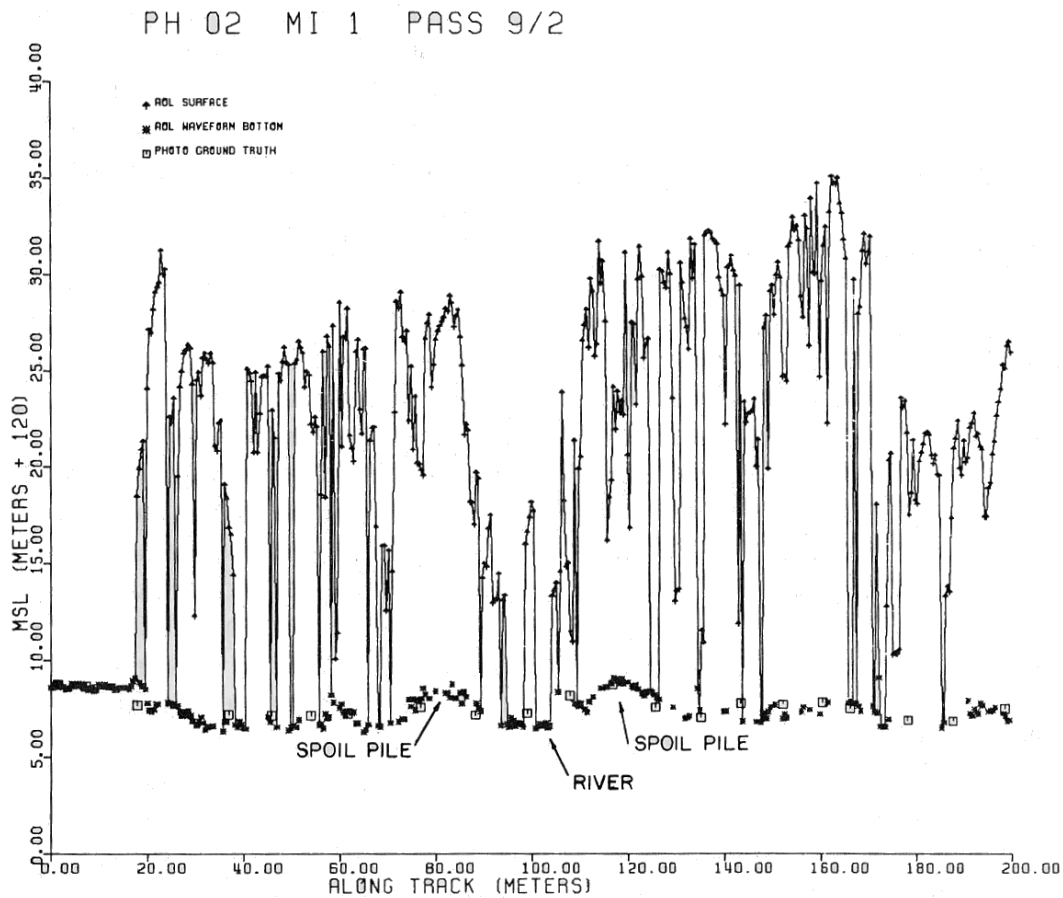


Figure 5. First measurements of terrain and trees from the NASA Airborne Oceanographic LIDAR (AOL) (From: Krabill et al., 1984)

NASA/Goddard Space Flight Center researchers have pushed the evolution of waveform and discrete return systems. NASA/GSFC developed the Scanning Lidar Imager of Canopies by Echo Recovery (SLICER), an airborne system, designed to describe the vertical structure of a tree canopy in the early 1990s. The LIDAR system developed for Mars (Mars Observer Laser Altimeter, or MOLA, 1996-2000) was limited by bandwidth, and hence was only a discrete return system. The MOLA technology design was subsequently flown as the Shuttle Laser Altimeter on the space shuttle in 1996 (STS-72), and 1997 (STS-85), and returned waveform data over much of the earth. Figure 6 illustrates the results taken from the Shuttle Laser Altimeter.

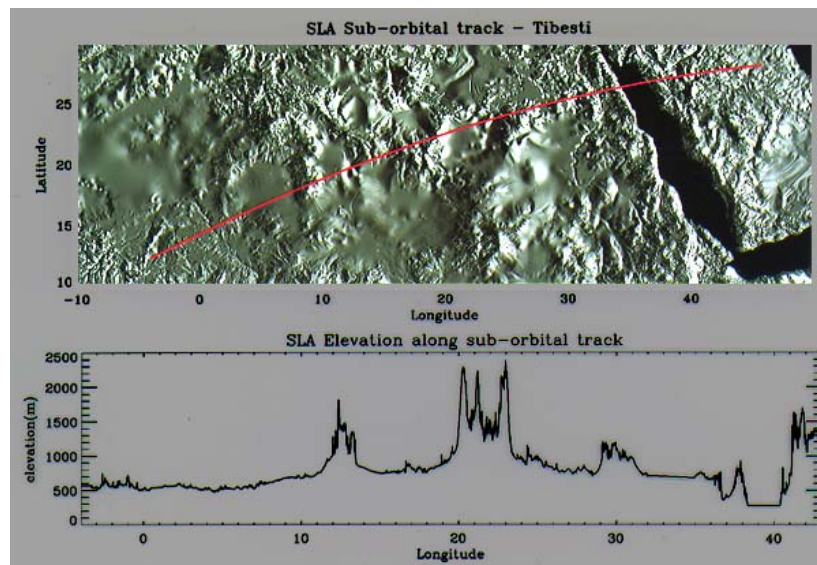


Figure 6. Results from the Shuttle Laser Altimeter (From: NASA, 2008)

The follow-on Laser Vegetation Imaging Sensor (LVIS) continues to fly in a variety of terrestrial environments. LVIS records the waveform returns and extracted forest features especially under canopies and characterized woodland areas (Hofton et al., 2002). During this period, algorithms for ground classification were developed using waveform analysis. These algorithms are now in use in the analysis of data from the following system, the Geoscience Laser Altimeter System (GLAS), carried on the Cloud and land Elevation Satellite (ICESat) (2003-2008) (Zwally et al., 2002).

The first operational airborne commercial FW LIDAR system appeared in 2004 (the LiteMapper-5600 LIDAR system), built by Riegl Corporation. Figure 7 illustrates the waveform data taken over various surfaces by the Riegl sensor.

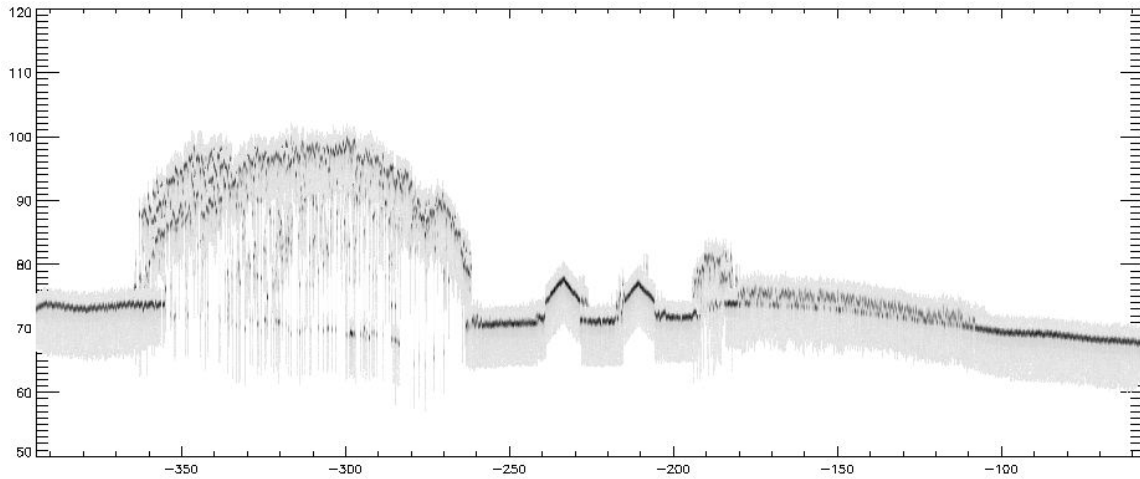


Figure 7. Profile 1 through forest, buildings, and corn field (From: Hug et al., 2004)

During the last two decades, comparisons of laser and other remote sensing methods, such as radar and optical sensors, have proved that lasers are among the best sensors for recording forest structure. High spatial resolution digital elevation models (DEMs) are gradually derived from LIDAR systems are also gradually being established as the most accurate such models.

C. PROCESSING FORESTRY LIDAR DATA

The following paragraphs are intended to provide an introduction of LIDAR remote sensing for vegetation applications (Lewis and Hancock, 2007). These paragraphs will also refer to the instruments and ideas currently used or that may have existed, and review features applications for exploring and monitoring vegetation.

1. Discrete Return LIDAR

In a discrete return scanning LIDAR system, the instrument is typically mounted on an aircraft (Figure 8), although ground based systems are also available. These systems examine the time it takes for each pulse to complete a round trip, hitting the

leading edge of the target (tree canopy top) or the trailing edge (laser beam penetrates canopy and hits the ground). These are referred to as the ‘first’ and ‘last’ returns.

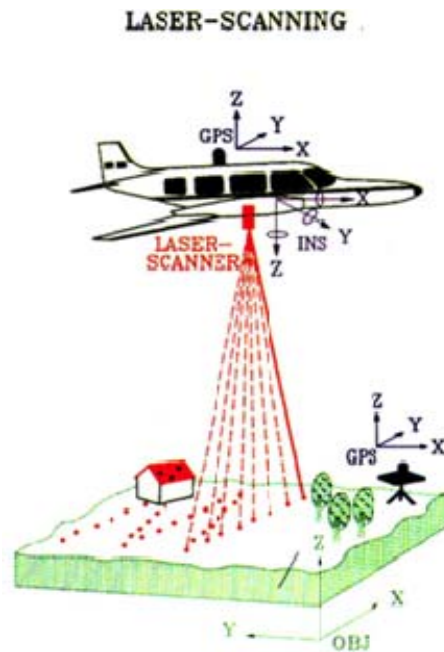


Figure 8. Typical airborne commercial discrete return LIDAR scanning system (From: Lewis and Hancock, 2007).

Although it is preferable to keep the footprint of the laser beam very small at about 10 – 30 cm to penetrate the canopy, it is possible for the beam to be completely absorbed by the canopy before it reaches the floor and/or may miss the tree tops (causing an underestimation of tree height). Tree height variance can be inflated due to misperceived tree heights within the tree height-finding model. Figure 9a shows correctly measured height for trees 1 and 3 because LIDAR returns intercept tree peaks (yellow). The height of tree 2 is incorrectly measured because the LIDAR return is from the side of the crown (blue). Figure 9b counts tree 4 as two stems (and heights) due to a forked or irregular tree crown.

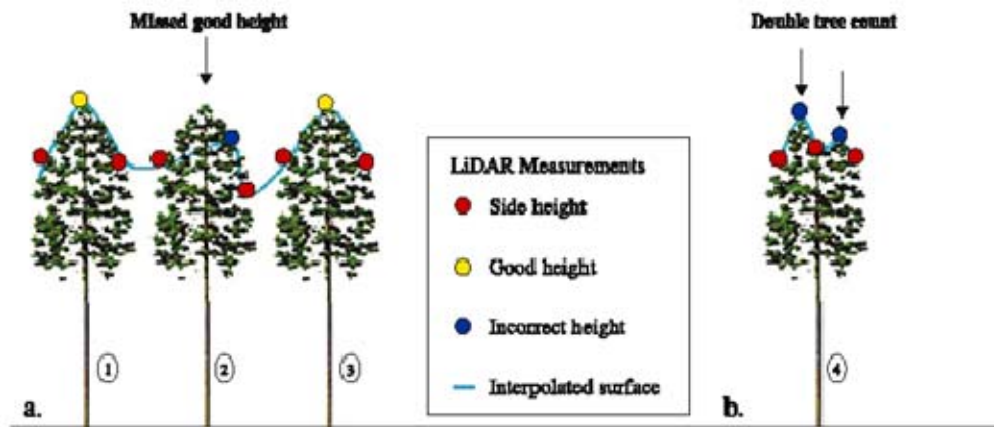


Figure 9. LIDAR misperceived tree heights measurements (From: Lewis and Hancock, 2007).

Since the sensors scan to get across-track spatial sampling (characteristically up to around 40°), the scan angle is an important tool to use to extract the tree height using the Pythagorean Theorem (Figure 10). LIDAR data formats generally provide 3-D results as $\{x,y,z\}$ triplets for the first and last pulse points.

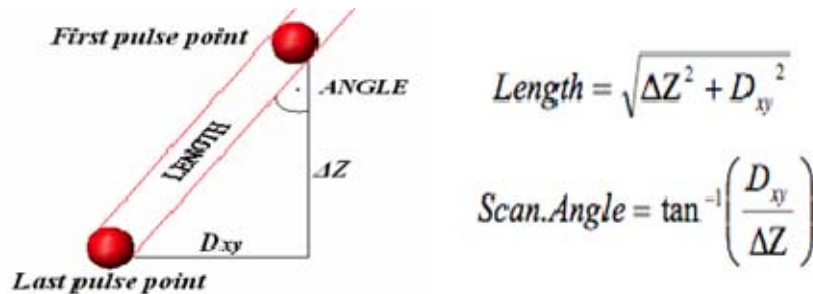


Figure 10. Angle effects on tree height measurements (From: Lewis and Hancock, 2007).

In this case, there are three reasons that can be used to explain the sources of the last returns: i) some returns of a large leaf or branch, ii) the slopes of the ground (Figure 11), and iii) shape of the understory (bushes or any kind of small trees close to the ground) that may complicate the recognition of a ‘ground’ signal.

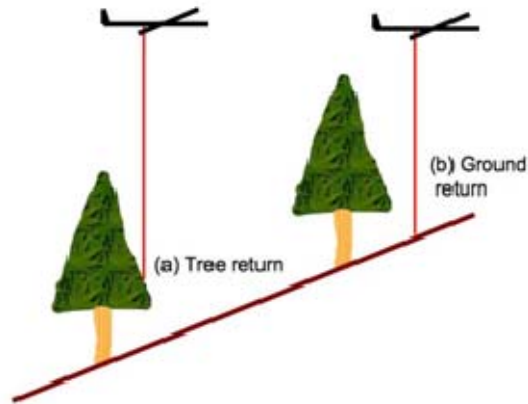


Figure 11. Slope effects (From: Lewis and Hancock, 2007)

A main characteristic of discrete return LIDAR systems is the intensity of the sampled signal for which the return may determine whether it is ground or crown. Figure 12 depicts the mean intensity of the LIDAR samples over a range of different age forest stands (Kalogirou, 2006). The ground-ground points are typically the highest intensity and the intensity of points that hit both crown and ground have the lowest intensity.

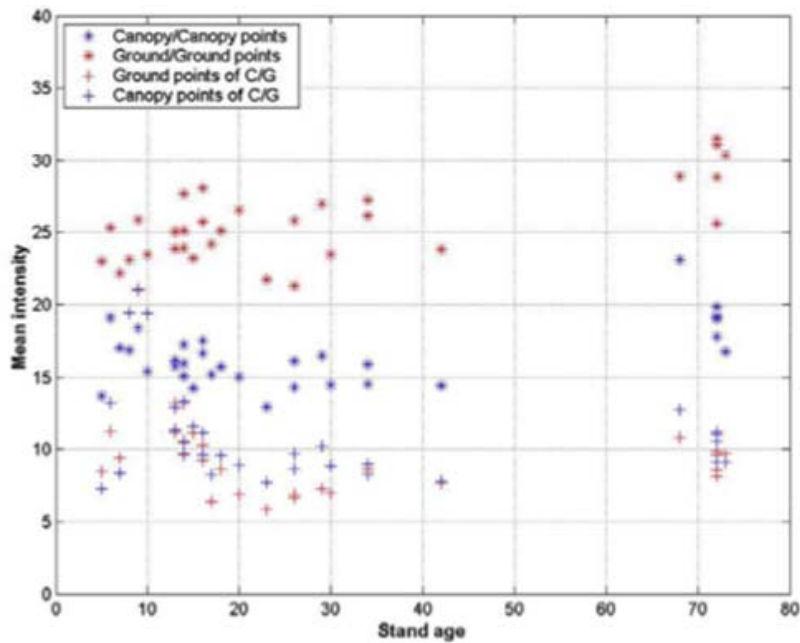


Figure 12. LIDAR intensity (From: Kalogirou, 2006)

The leaf reflectance is generally higher than soil reflectance in the near infrared so it is expected that the return from the leaves should be higher than that from the ground. However, this does not occur because the leaf causes more laser beam scattering than the ground. The proportion of radiance viewed by the sensor is relatively small and reflected energy from only a portion of a canopy is measured. Additionally, the ground is relatively flat, resulting in a strong ground return (compared to leaves).

A recent operational airborne platform system is the Optech ALTM 3033 LIDAR flown on a Piper Navajo Chieftain aircraft run by the Unit for Landscape Modelling at Cambridge University. It collects 33 kHz in standard operating mode and measures first and last returns and intensity data. The RMS accuracy of the height data is ± 15 cm, from an operating altitude of 3000 ft.

2. Waveform LIDAR Systems and Analysis

In a waveform LIDAR system, the system samples and records the returned energy for equal time intervals ('bins'). Such systems are reliant on relatively new technology. Existing waveform LIDAR systems typically have a much larger footprint than discrete return systems, working with footprints on the order of tens of meters.

A large footprint is used in waveform LIDAR for forestry applications because there is a greater chance that some signal will be received from both the top of a tree and the ground. This makes it possible to measure some characteristics of a whole tree or several trees (Figure 13 and 14), where the amplitude of the reflected laser energy shows features relating in some way to the measured features of the tree. The example in figure 13 depicts two main peaks: one associated with the crown and one from the ground signal. The trade-off is that the local ground slope, at which the LIDAR can be used, decreases with increasing footprint size. If the slope is too high, then it is more likely to have a mixed signal for higher slopes for canopy.

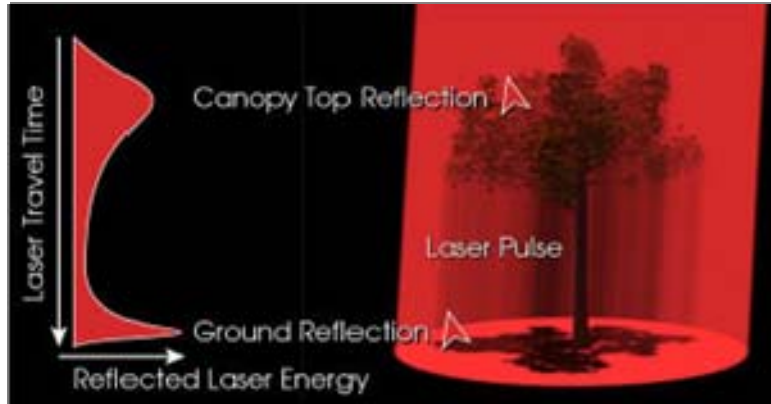


Figure 13. Waveform LIDAR Operation (From: Lewis and Hancock, 2007)

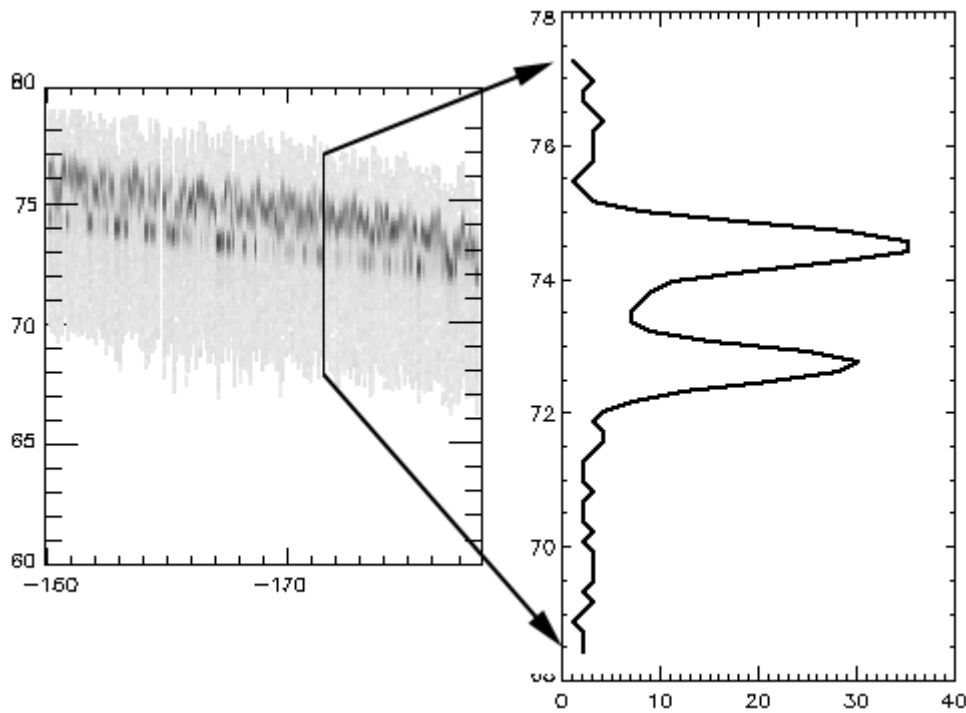


Figure 14. Riegl LiteMapper 5600 data from a Corn Field (see also Figure 7 above) (From: Hug et al., 2004).

One of the first airborne small-footprint waveform digitizing laser scanners is the RIEGL LMS-Q560 (http://www.riegl.com/uploads/tx_pxprigldownloads/lms-q560_datasheet.pdf). It enables the user to analyze the data during post-processing and extract additional information from the data. The number of pulses, the pulse width and the amplitude are used to classify the vegetation points.

Figure 15a depicts a 3-D point cloud of single returns, while Figure 15b shows the multiple returns, which are important in filtering and modeling algorithms related to vegetation and ground surface separation, as well as forest parameters.

The amplitude of the returns of the digitized data is a very important factor, from which very important information about the structure and texture of the target can be extracted. It is possible to discriminate between surface objects based on their amplitude (Figure 16a). Also, in combination with the range, a visualization of the scene and separate the objects can be created. The amplitude for classification cannot be used because sometimes the amplitude of different objects matches each other (for example, a grass slope and asphalt street). In order to distinguish between objects and especially vegetation, the pulse width is needed. Broader pulse width corresponds to vegetation. Figure 16b illustrates a cloud of points classified as vegetation and non-vegetation points based on their pulse width (dark points correspond to vegetation).

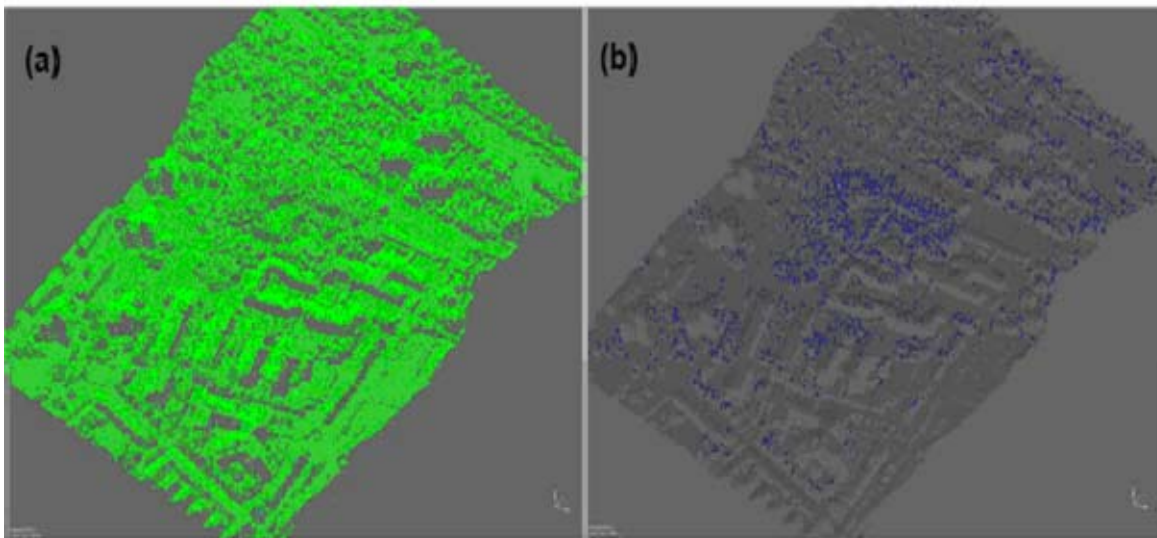


Figure 15. 3-D point cloud of the study area. The color shows the index of the corresponding scatterer. (a) Points presenting only one echo pulse are in green. (b) Points presenting two echoes and more are in grey and blue (From: Ducic et al., 2006)

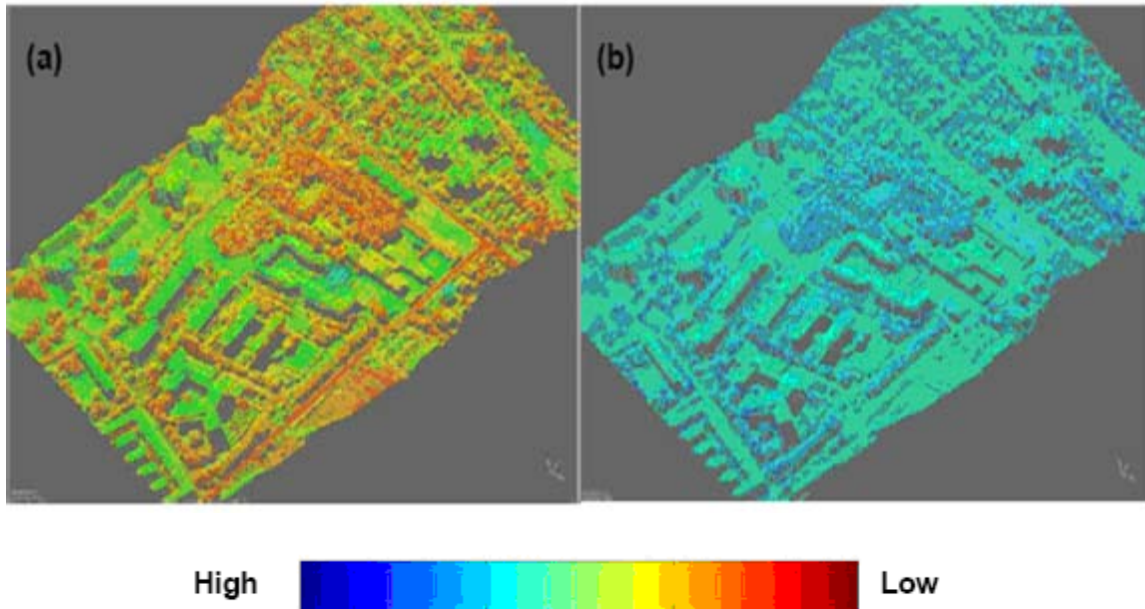


Figure 16. (a) Amplitude image showing trees, vegetation, access roads and buildings. (b) Pulse width image (From: Ducic et al., 2006)

Means et al. (1999) describe early waveform data taken with the SLICER instrument in 1995. This early system had a very low repetition rate (80 Hz), but it could be flown at relatively high altitudes and has a Horizontal positioning accuracy of around 5-10 m (Figure 17).

SLICER RETURN PULSE WAVEFORM

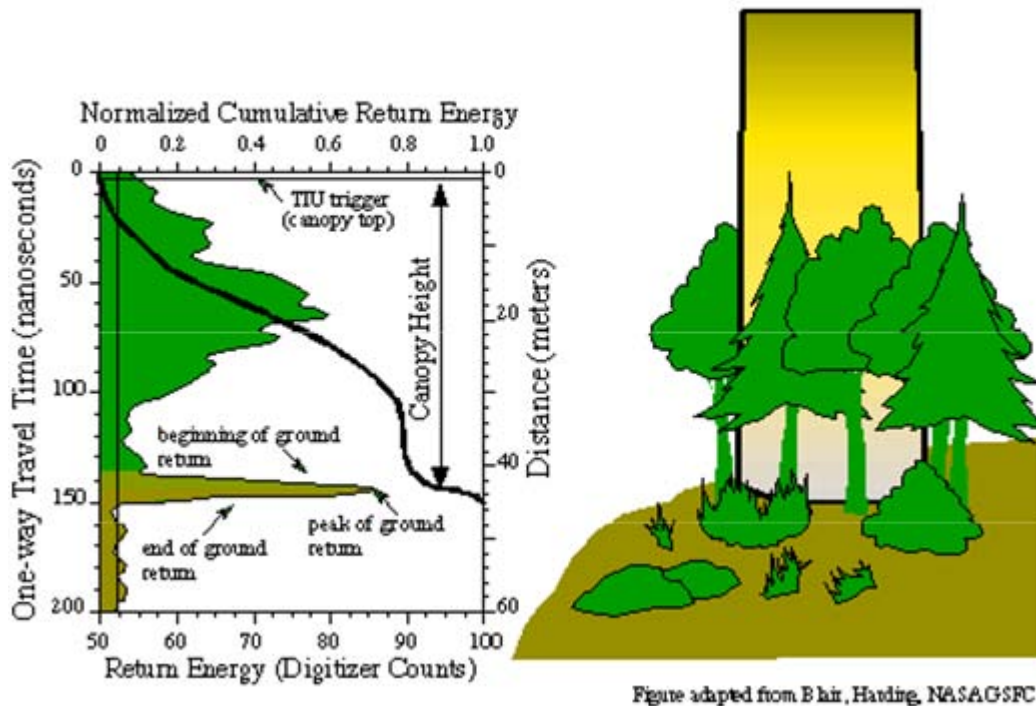


Figure 17. SLICER operation (From: Dubayah et al., 1997)

The vegetation canopy LIDAR (VCL) (Dubayah et al., 1997), was the initial NASA/GSFC design for a space born instrument to measure global characteristics of forests. Construction was nearly completed; the system failed to be launched into space due to programmatic issues. This technology was applied to the IceSat Geoscience Laser Altimeter System (GLAS), launched in 2003. With a 70 m footprint, a ground slope over 10° complicates the ability to retrieve canopy information. Comparison to a smaller footprint system such as the 25 meter footprint LVIS system shows an apparently small effect from the footprint size, so the error caused by slope is insignificant compared to other experimental errors (position, multiple scattering, Gaussian energy distribution across footprint).

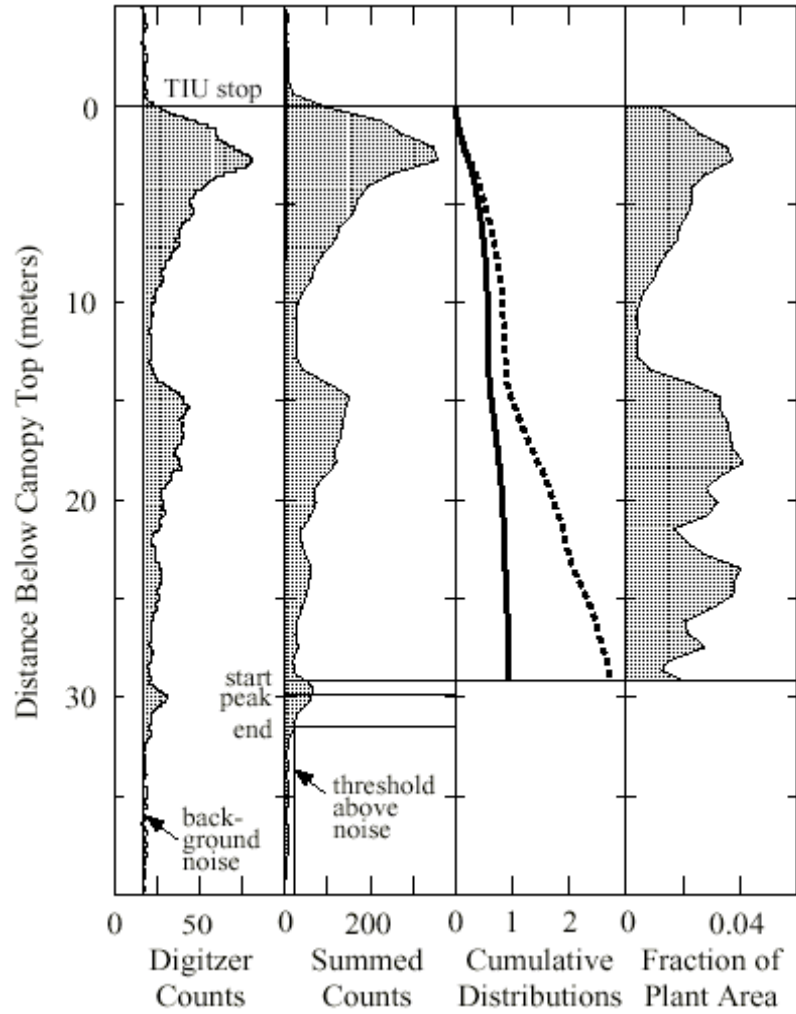


Figure 18. Steps in converting a raw SLICER waveform to various processing levels. (From: Progress in Lidar Altimeter Remote Sensing of Stand Structure, In Deciduous and Coniferous Forests Using Slicer Data; Michael A. Lefsky, David J. Harding, Geoffery G. Parker, Warren B. Cohen, Steven A. Acker; Proceedings of the ISPRS Workshop; Mapping Surface Structure And Topography by Airborne and Spaceborne Lasers; November 9-11, 1999; La Jolla, CA; ISPRS WG III/5: Remote Sensing and Vision Theories for Automatic Scene Interpretation; ISPRS WG III/2: Algorithms for Surface Reconstruction; International Archives of Photogrammetry And Remote Sensing; XXXII-3/W14 (<http://www.isprs.org/commission3/lajolla/>))

The next airborne waveform system from this group is known as LVIS (Laser Vegetation Imaging Sensor) was developed by NASA (NASA, 2008). The laser scan can be adjusted by software in real time to remove forward motion effects and platform angle

changes. Data on the surface below these swaths are collected, and a Digital Elevation Model (DEM) and map can be generated from them. LVIS has a scan angle of about 12 degrees, and can cover 2 km swaths of surface from an altitude of 10 km (Figure 19).

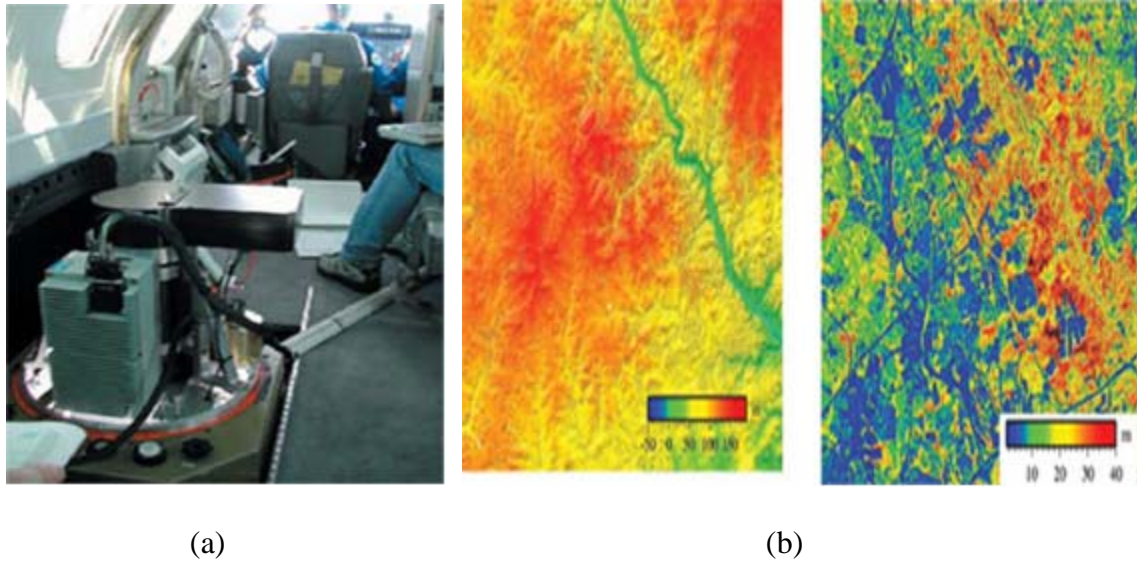


Figure 19. (a) LVIS can be mounted on any aircraft that has a standard aerial camera mount and a window. (b) These sample data show bare-earth topography for an urban and forested region in central Maryland, collected in leaf-on conditions. Above right: Vertical extent of vegetation and buildings in the same region of central Maryland. Blue areas are flat (i.e., roads), and yellow and red areas are tree heights ranging from 25-30 meters.

3. LIDAR Data Extracted Information

A huge variety of techniques and algorithms are used to analyze LIDAR data to derive tree characteristics and other under canopy information. All the characteristics may generally be derived from either discrete return or waveform, in which it is possible spot the signal features coming from the top or under the canopy.

One technique used by the GLAS team estimates tree or canopy height by measuring the top five tree heights in a forest to extract information for all tree species around the area (Lefsky et al., 2005). It uses a large footprint LIDAR, which makes it difficult to identify particular trees for validation; nevertheless, this is often executed in some local average measurements (e.g., stand scale in plantations). In the case of non-

plantation forests or rainy forests, canopy structure can be very complex and so there can be noteworthy local variation in tree height. However, in most cases, LIDAR can provide almost direct measurements of tree or canopy heights.

An advantage of waveform LIDAR is the use of statistical analysis, which helps to determine the vertical distribution of foliage and branch matter. This technique requires some form of model (making particular assumptions relative to the angular distribution and spatial organization of the scattered light). To make single tree extraction, Brandtberg et al. (2003) used a method of gradual coarsening of vertical resolution. After the number and height of trees was determined, the 3-D appearance with bark reflectance was combined to get accurate species determination.

Full waveform laser scanning offers the capability of automatic classification of points (Ducic et al., 2006). Prior to determining the signature of the objects, 5000 training points were chosen to do the signature analysis for the classes: vegetation (trees and bushes), grass, asphalt road and various roofs (buildings and houses). Two different lists of histograms were created (Figure 20) one for pulse width (a) and one for the amplitude (b) and they initially observed that the multiple echoes correspond mainly to vegetation points. It can be seen that there is an overlap in the amplitude-pulse width space for different classes and cannot be made classification reliant only on one of the two features of the waveform. In order to define a decision tree algorithm such as vegetation or non-vegetation, we can combine the two different features plus the range and multiple returns of the target.

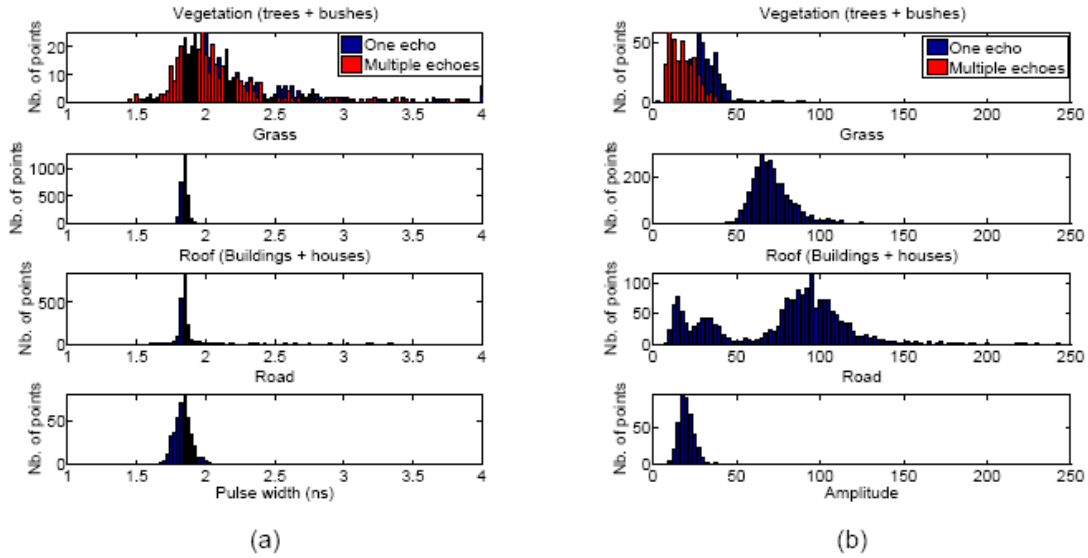


Figure 20. (a) Histogram of the pulse width of points. (b) Histogram of the amplitude of points. The blue points correspond to one echo and the red ones to multiple echoes. (From: Ducic et al., 2006)

Waveform LIDAR systems are more capable of deriving information about canopy structures and tree characteristics. New technology in airborne LIDAR instruments and an increasing variety of them over past years, allows the expanded capabilities of LIDAR in many applications such as measuring vegetation canopies. Unfortunately, no space borne LIDAR systems currently exist that are specifically designed for measuring canopies besides some efforts by the VCL.

4. Discrete Returns vs. Waveform Data

It is possible to compare the structure of the returns in the two existing forms: the discrete returns and waveform. Figure 21 visualizes different cases of possible target situations and shows the difference between the discrete interpretation and the actual waveform of the backscattered echo. It shows the differences between the two types of returns. While the discrete returns analysis shows the range (the first and last returns) and the reflectivity of the target (by analyzing the amplitude of the discrete pulse), the waveform analysis shows the texture of the target and also the situation of the target in respect to the scan angle of the laser beam. Therefore, Figure 18 shows a broadening of the echo's pulse when there is a slope on the ground. Finally, multiple returns in

waveform analysis can illustrate the texture of the target and give more accurate classification of the data. A careful consideration of both types of data can provide an exact 3-D image of the forest classification.

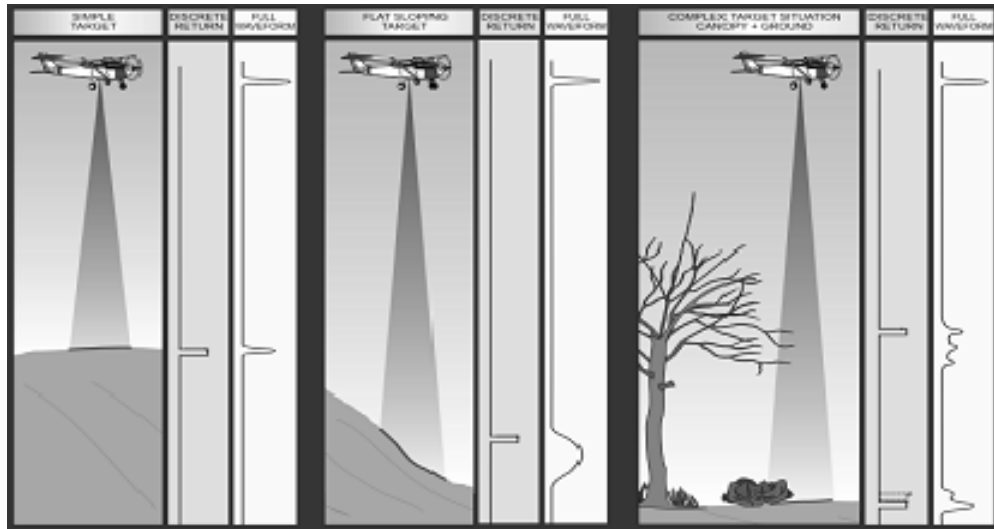


Figure 21. Echo signals from different target situations. For every target type from left to right: sketch of target and laser beam, discrete return result, full waveform echo signal.

So far, ALS systems have provided only specific types of 3-D coordinates, compelling discrimination and classification approaches to rely on discrete returns only. Full-waveform laser scanners supply quality tools as pulse amplitude or pulse width, which can be used to expand upon the classification steps further. On the other hand, comparison with discrete returns improves the visualization of the data. The classified vegetation points are used to create digital terrain model (DTM) and digital surface model (DSM) products, which are particularly useful for forestry applications.

D. LIDAR BENEFITS

There are many advantages when using LIDAR. These include large area coverage in a short time period, high levels of accuracy, reasonable cost considering other conventional collecting data and portability.

The most noticeable benefits of LIDAR over conventional photogrammetric data collection include efficiency involving point density and time saving. Most LIDAR devices can collect 10,000 mass-points per second, while the conventional stereo compilation techniques can collect only approximately 0.4 points per second (Prasad, p. 7).

Multiple returns by the LIDAR system cover almost 24 points per m², resulting in a better 3-D representation. Imagery and 3-D visualization give more/have a higher level of confidence, while mapped images better represent the actual existing conditions. Additionally, it can map both bare earth and split ends of terrain among high vegetation. The filtering procedure also allows 'unclassified' data to be gathered to analyze tree canopy and contour line-of-site, as well as measure power lines.

As an active and portable sensor, LIDAR can be moved easily, data collection can be done quickly and data retrieval is not limited to daylight hours (Emison, 2008). Measurements do not depend on the sun's position or inclination and surveying can be accomplished at any time (Figure 22). The precision of data gathering is slightly affected by the weather, but clear weather conditions offer more reliable results. Even most risky, hard to reach, or prohibited areas can be accessed for mapping by air.



Figure 22. Laser radar beams light up the sky on a winter's night at the LIDAR Research Laboratory in Chatanika, Alaska as part of an international collaborative study of the polar atmosphere. (From: Emison, 2008)

Digital technology allows fast and automatic delivery/turnaround progress, eliminating film scanning and reducing human work hours. The majority of the LIDAR data capturing requires very little user input. Data loss is less of a problem, and additionally, other flights record areas where points had previously not been collected. Besides, direct digital acquisition provides almost 95 percent forward lap between exposures within a flight lines. It is noticeable that such a large percentage number allows up to 9-10 deferent analyses of the same feature.

LIDAR's function typically consists of the integration of three different technologies into a unique system, capable of producing accurate DEMs by using the appropriate data. GPS, lasers and inertial navigation systems combined allow a high degree of accuracy in the footprint positioning of a beam when it hits an object. The accuracy of lasers is generally a few centimeters; therefore, the LIDAR's accuracy limitations are due essentially to the GPS components. Improvements in commercial GPS and inertial measurement units have already lead to the increasingly high accuracy level using LIDAR from helicopters or wing-fixed aircrafts. Compared with the orthophoto technique, LIDAR is much more accurate in foliage; ± 15 cm horizontal and ± 10 cm vertical, while the orthophoto technique faces problems with the projection on slopes and shadows from tall trees. With a special interpolation and filtering process, it is possible to obtain higher post spacing intensity. It is, therefore, feasible to detect small changes in the landscape. This application is enhanced by the elevation information, a feature of which conventional orthophotos are not capable.

Preliminary results in a South San Francisco Bay survey pointed out that, in small areas, when LIDAR is compared with photogrammetry, LIDAR techniques provide more accurate data. (Foxgrover and Jaffe, 2005, p. 8).

As shown in Tables 1 and 2, the vertical accuracy of the measurements throughout the study area on hard surfaces is 0.1 to 0.15 m for LIDAR, while the horizontal accuracy varies between 0.2 and 0.6 m.

Error (LIDAR) (cm)	Error (Orthometry) (cm)	Terrain Description
+/- 10 – 15	+/- 15 – 30	Hard Surfaces (roads and buildings)
+/- 15 – 25	+/- 25 – 40	Soft/Vegetated Surfaces (flat to rolling terrain)
+/- 25 – 40	+/- 35 – 50	Soft/Vegetated Surfaces (hilly terrain)

Table 1. Absolute vertical accuracy.

Error (LIDAR) (cm)	Error (Orthometry) (cm)	Terrain Description
+/- 20 – 60	+/- 30 – 60	All locations except extremely hilly terrain.

Table 2. Absolute horizontal accuracy

An advantage of LIDAR versus other analog techniques is the included multispectral data. The ability to allow users to acquire RGB, panchromatic and color IR data from one flight is significant. One analog camera would need to be airborne on top of the projected area in three separate flights to provide an image similar to that of LIDAR. Typically, additional data collection from air would be expensive and possibly not affordable. While many clients may not recognize the benefit of multispectral data, it has proven to be useful for land/vegetation delineation, under canopy surface identification and wildfire hazard evaluation. Several useful models were used in Wyoming's Casper Mountain area where multispectral data was implemented for wildfire hazard assessment and allowed professionals to develop land classifications and diseased plants calculations to help identify fire risk areas (Caldwell, 2005).

E. WHY LIDAR?

Remote sensing can be basically defined as the action of evaluating some aspect of an object either, small (plants) or large (tree, road, trail) from a different location. Many disciplines use these techniques, especially the atmospheric science discipline. The first tools of remote sensing included balloons and rockets, followed by radar and after World War II, LIDAR was discussed and used.

The use of LIDAR in forestry and road construction applications is a major task. For this reason, forest ecological companies use high-accuracy LIDAR data from air for optimization of roads and trails, as well as forest inventory and monitoring. More data of the terrain topography provide a better chance to make a more effective transportation route or protect the environment against natural changes (LIDARcomm).

Collecting aerial LIDAR data is a safe, unobtrusive and environmentally friendly method. Unlike other ground analysis procedures, airborne LIDAR can collect data over limited, undesirable, or inaccessible areas. Apart from the necessity to certify the LIDAR measurements with ground truthing, no need exists to send pervasive crews to conduct deep survey operations. LIDAR surveying in forest or low visibility areas can avoid needless tree cutting or other practices, which can harm the environment.

In addition, many types of information can be shared that will be practical and helpful to conservationists. Scientists will be able to gather all LIDAR maps and identify areas which areas that are most vulnerable or recognize dense plants and tree canopies to allow them to mature into the majestic groves of this world (Rowe, 2007).

F. LIDAR ACCURACY AND ERRORS

1. Accuracy

The purpose of this section is to provide necessary information and discussion points for LIDAR users to better understand the term of LIDAR accuracy specifications, because each user will be faced with various interpretations – and misinterpretations – of what is meant by the accuracy of the LIDAR data. LIDAR system manufacturers are often not going to reveal the conditions under which system specifications apply and they generally know how to present the best results. There are also different interpretations of common terms due to a lack of clear definitions.

The published documents about LIDAR accuracy specifications generally provide little information on how this accuracy is measured. As illustrated in Figure 23 some critical information such as operating altitude, full or limited scan angle, target type and slope, GPS quality required to reproduce, etc. is often not included. Some key points from Airborne 1 Corporation in respect to LIDAR accuracy are cited.

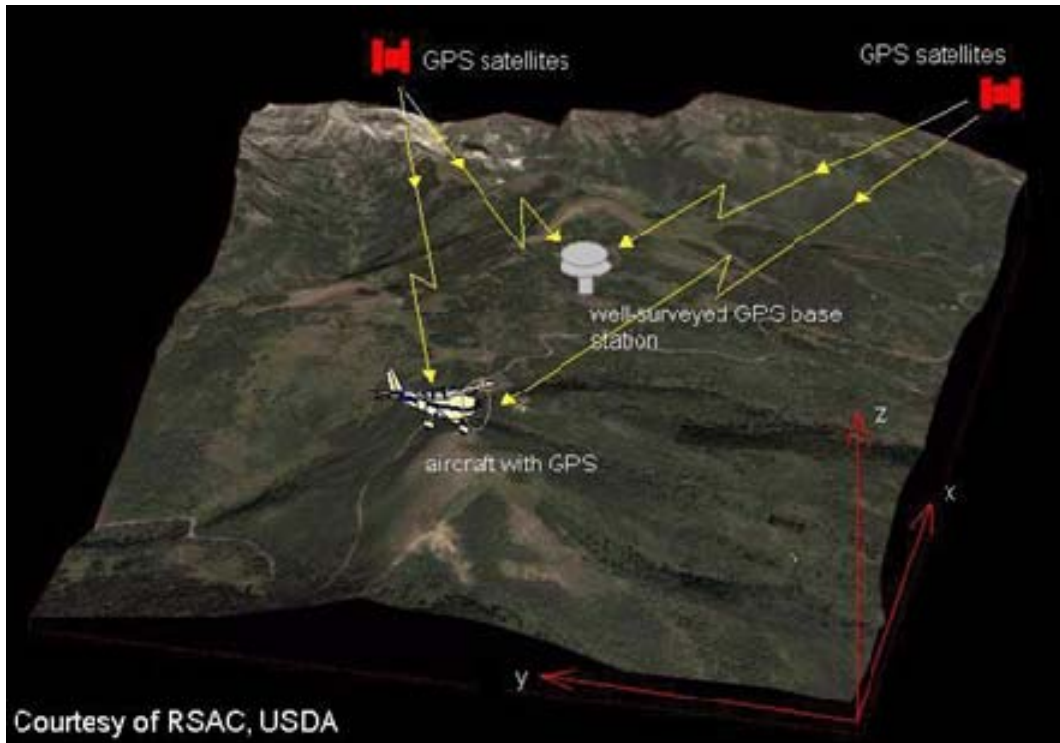


Figure 23. GPS communication with LIDAR system (From: www.forestry.gov.uk)

Manufacturer's accuracy specifications are derived from statistical sampling of the LIDAR data and are generally quoted as a 1 sigma spec, meaning ~68% of the data will fall within or 90% (1.6 sigma) specifications are generally not mentioned.

Accuracy specifications are generally taken across the entire scan width of a system despite the fact that accuracy will decrease with increasing scan angle; it is common to see the quoted accuracy being the average of the error at minimum and maximum scan angles.

Accuracy is generally taken in the GPS reference frame so effects of geoid modeling are ignored. Accuracy analysis is generally taken by comparing to known ground control points, but details of how this was done are generally not included.

Accuracy analysis tends to focus on vertical accuracy (Z) and details on how planimetric accuracy (XY) is verified are vague.

2. Errors

The total inherent errors are comprised of the contribution of errors of each subsystem of LIDAR components and the final operational accuracy that can be achieved is generally worse than the theoretical limit. The accuracy of the final digital terrain model accuracy is the result of a combination of different inherent error sources in the acquisition and errors due to the processing procedures. The primary inherent error sources of a LIDAR system during acquisition process are as follows.

a. Laser Rangefinder Error

Laser rangefinder is a well known technology that measures the distance that based on the time delay of each pulse between the LIDAR and the target. Under normal operating conditions, the range error from a properly calibrated laser is about 5 – 7 cm, independent of altitude. However, proper calibration does not eliminate some parameters that affect the final results, such as the timing jitter in the on-board clock, the relative position of the system in respect to the target during the transmission and receipt of the pulse or errors due to bounce of beam between branches and bushes. In addition, atmospheric effects can impact the accuracy of the laser rangefinder, especially at higher altitudes. Proper tuning of the laser's beam wavelength can reduce the effects. Moreover, people introduce an atmospheric model that usually minimizes the effects in the post-processing of the LIDAR data.

Another issue to take into consideration regarding the rangefinder is the divergence of laser beam as it propagates. For example, an output beam with a spot size of 0.1 cm and a divergence of 0.25 mrad as it exits the sensor will illuminate a footprint on the ground of ~25 cm from an altitude of 1000 m and ~50 cm from 2000 m. Therefore, for small footprint, it is necessary to consider the footprint size when taking into account accuracy.

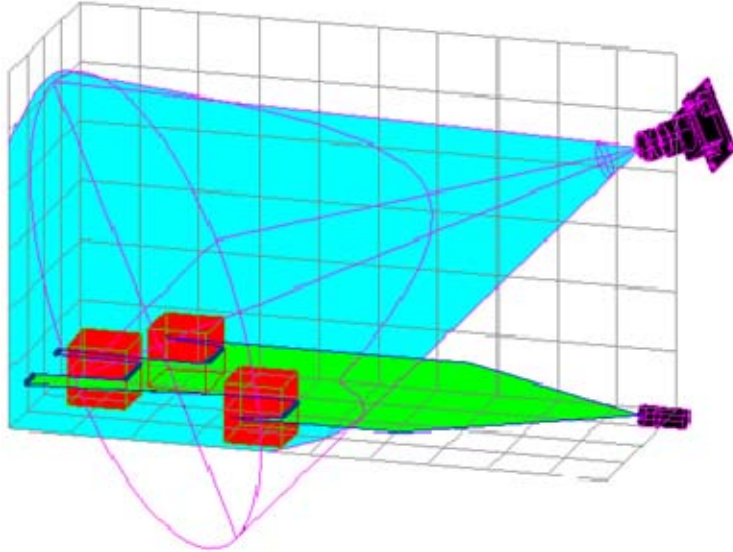


Figure 24. This figure demonstrates how a single coherent beam of laser light is diffracted into an angular field. An error can occur due to geometric relationships imposed by axial mounting considerations between the camera and the laser field generator

The returns from the target are a combination of the energy transmitted and received from the system as well as the ground slope across the footprint. At higher slopes, only small amounts of radiated beams return to the sensors.

b. GPS Positioning Error

GPS errors are divided in two basic categories: the inherent GPS errors and ground control errors. The first category includes carrier phase GPS positioning errors. These errors are the same for each user and vary from centimeter-level accuracy to one meter-level accuracy. Some factors are: satellite geometry, the number of satellites, orbital biases, multi-path, antenna phase center modeling, integer resolution, and atmospheric errors. The second category of GPS errors is the accuracy of geoid height models. GPS heights are relative to an ellipsoid. Nationally, the current geoid height model (GEOID99) has a precision of ± 5.2 cm (1s) at a 5-km distance. Therefore, any vertical GPS error, such as geoid height modeling, will directly influence the accuracy of any LIDAR product.

c. IMU Orientation Error

The IMU is used to determine the aircraft attitude in terms of pitch, yaw, and roll, the vertical and horizontal movements of the aircraft in flight (Figure 25). Accurate measurements of the platform orientation are required to determine correctly the pointing direction for each laser pulse relative to Earth surface coordinates. IMU is hard mounted to the LIDAR sensor and the errors are derived from the scanning subsystem. These can be described with respect to the scanner mirror angle and laser pointing errors (Nayegandhi, 2007). Some of these errors can be reduced by proper system calibration prior to data collection and proper system modeling during post-processing. It is necessary to keep in mind that, when considering final achievable accuracy for the LIDAR sensor, system engineers must consider the entire error budget and not simply focus on the IMU.

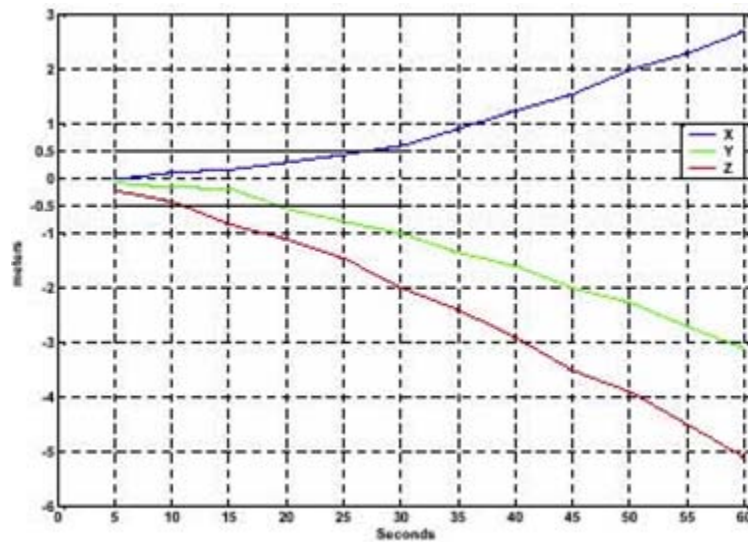


Figure 25. Error in IMU-derived position. The diagram shows the error in the position derived from the stand-alone IMU for one minute

d. Filtering Processing Error

Filtering Processing Errors occur because of vegetation noise (inability to penetrate heavily canopied forests without breaks, thus preventing creation of accurate DEM). Bare Earth under short grasses is much harder to determine (dead zone effect). An

error depends on the type of surface being mapped and ranges from a few centimeters in open canopies to up to several meters in closed canopies and sloping terrains.

e. Errors in LIDAR Ground Elevation and Wetland Vegetation Height Estimates

(1) Ground Estimation. For some LIDAR systems, it is difficult to record ground returns in areas with dense ground vegetation. Therefore, an overestimation of ground height occurs due to minimal pulse penetration.

(2) Canopy Height. In dense forests, due to the reason in (1), in addition to the attribution of penetration of laser beam into the foliage (no returns from tree top), an underestimation of canopy height can be made. The largest absolute errors in the estimation of LIDAR canopy surface height were associated with tall vegetation classes. However, the largest relative errors were associated with low shrub (63%) and aquatic vegetation (54%) classes. Also, it is difficult to obtain returns from non reflective materials, such as water and black surfaces.

(3) Position Errors. Position Errors can occur in the DEMs (Digital Elevation Models) and CHMs (Canopy Height Measurements), because all generated surfaces are a smoothed representation of the true surface. Attempts are made to keep the error (or misrepresentation) to a minimum. A great deal of research is currently being channeled into developing superior DEM generation algorithms for this purpose, particularly in steep and heavily wooded terrain (Woodget et al., 2007).

(4) Scan Angle. LIDAR errors can occur due to the scan angle of a LIDAR beam. Generally, scan angle varies from 15° to 50°. The wider the scan angle the less accurate the results will be due to lesser numbers of light pulses reflecting upon the earth's surface. Many studies have found errors associated with both DEM generation and canopy height estimation (Figure 26) to increase with increasing scan angle (Ahokas et al., 2003). It is anticipated that this results from a lower intensity of reflectance at greater scan angles, as dictated by Lambert's Cosine Law.

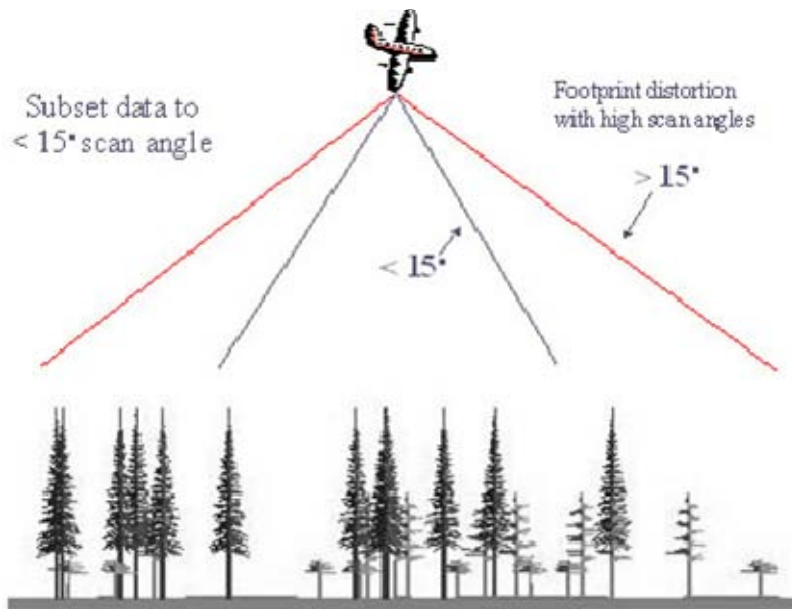


Figure 26. The scan angle must be within 18° of nadir; otherwise, LIDAR footprint can become highly distorted (From: www.cnrhome.uidaho.edu)

Higher numbers of pulses per unit area can be achieved with the following methods: i) slower aircraft speed, ii) lower flying altitude, iii) reduced scanning angle, and iv) increased pulse emission.

(5) Flying Altitude. At greater altitudes, lower density returns occur (Goodwin et al., 2006; Takahashi et al., 2007), due to the larger distance between sensor and target. This causes a reduction in the intensity of the return pulse in accordance with Newton's Inverse Distance Law. In case the intensity falls below a certain threshold, the pulse becomes indistinguishable from random noise, and therefore, is not recorded. This is much more likely to happen at greater flying altitudes. Furthermore, recent work by Takahashi et al., (2007) demonstrates that an increase in both systematic and random errors of mean tree height estimates is observed with increasing altitude. Consequently, a flying height of less than 1000 m for tree height studies is recommended.

G. LIDAR APPLICATIONS

Each application itself has explicit demands, for spectral, spatial and temporal resolution. There can be many applications for LIDAR, in different fields, as described below. In the body of LIDAR benefits, some of the most important applications will be mentioned for civilian and military purposes.

1. Civilian Applications

a. Geology-Seismology

In geology and seismology, LIDAR technology and GPS have evolved into the study of earth's structure to realize the grandness of earth's physical crustal processes. Considerable natural disasters such as hurricanes or earthquakes lead into airborne laser mapping development which allows timely and accurate survey data to be collected and rapidly assessed. This combination was also used to create accurate elevation models for territories, measure ground elevation under canopy and also to find the location of the Seattle Fault in Washington, USA (Figure 27).



Figure 27. The Seattle Fault between Puget Sound and Seattle.

b. Forestry

The use of airborne LIDAR in the forestry industry started early and has become widespread. Conventional techniques did not suffice to obtain critical and accurate information such as densities and tree heights. Airborne LIDAR technology can produce a mapping image of the ground under canopy, while simultaneously mapping tree heights. Such accurate information on the topography and terrain beneath the tree

canopy is very important to many industries including forestry, energy, railroad and also to natural resource managers (Airborne Laser Mapping). Of the utmost importance is that forests play an essential role in balancing the Earth's CO₂ supply and exchange, being the key link between the atmosphere, geosphere, and hydrosphere (Figure 28).

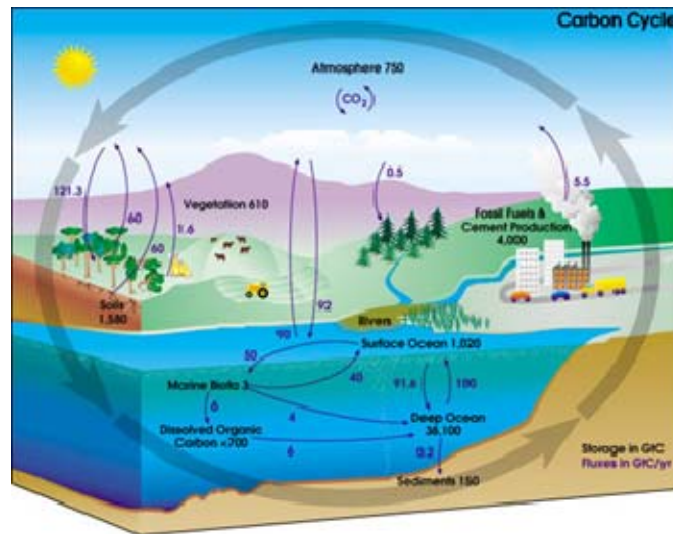


Figure 28. Total amounts of stored carbon in black, and annual carbon fluxes in purple. (From: NASA Earth Science Enterprise)

c. *Sea Ice*

Ice covers a considerable part of the Earth's surface and is a key factor in global climate change studies and commercial shipping industries. Airborne LIDAR altimetry provides a direct geometry measurement of an ice surface with an accuracy of 5-25 cm, thus providing a useful estimation and validation tool for sea-ice thickness measurements. The LIDAR measurements are based on accurate GPS positioning attitude data in combination with a geoid model and its precision is currently limited by long-range kinematic GPS performance. Figure 29 shows the Geikie operations that occurred between 1996-98, which included repeated GPS measurements and mapping by airborne LIDAR altimetry at the top of the Geikie Ice Plateau, East Greenland (Forsberg, R. et al., 2003). Some other similar applications include iceberg detection and tracking, ice condition and ice type/age/motion evaluation.



Figure 30. The photo above shows the 0.1 ft. RMSE accuracy of the 20-mile corridor project T-REX, Denver, CO in 2000.

In topographic mapping, multispectral imagery as a component of LIDAR technology provides ancillary terrain information for forest cover and supplements data with the textural nuance inherent in LIDAR imagery. With this, a composite image product useful for interpretation can be created (Uddin).

e. Oil and Gas Exploration

LIDAR data has several potential applications in industries such as oil and gas exploration, as well as the exploration of other natural resources. The high-resolution features of LIDAR provide all of the necessary tools to engineering organizations in an extremely time-sensitive manner. It offers extremely accurate terrain models and imagery for ground verification. All LIDAR data sets produce high-resolution, three-dimensional imagery and local mapping, which reduces the expense of costly ground surveys.

f. Corridor Mapping

Airborne laser mapping allows truthful and rapid mapping of linear corridors, such as gas pipelines, railways, highways, or power utility right-of-ways. A helicopter bound LIDAR sensor can be used for the mapping of a corridor by flying at lower altitude to collect accurate and dense data of corridors. These data are useful in

setting up the corridor and during execution of work. Even without extensive cost-benefit analysis, it is possible to monitor the deflections and possible areas in need of repair at a later time.

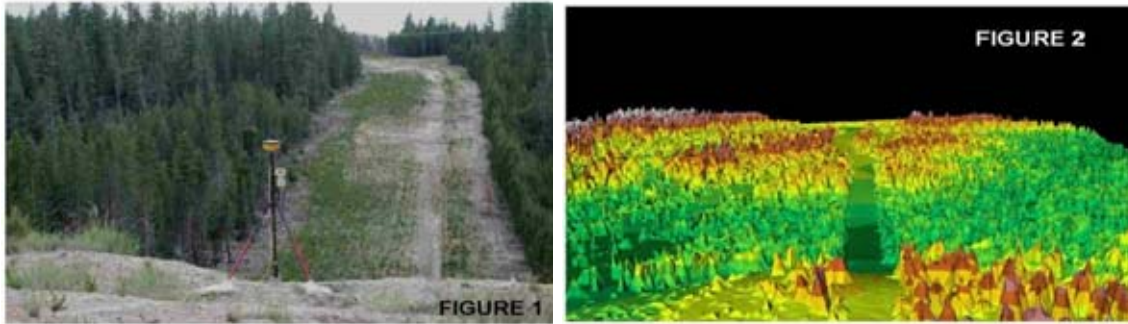


Figure 31. Corridor picture analyzed and converted to LIDAR data imaging

g. Flood Plain Mapping

Applications for LIDAR mapping services also include floodplain mapping. Airborne LIDAR mapping is the faster and most precise method to obtain three-dimensional data suitable for producing high-resolution digital elevation data for flood and inundation risk management. Many task forces have found that current methods of high risk areas mapping was inadequate for the analysis of flood risk, or for the consideration of inundation protection options. This was the reasoning behind some planners' and hydrologists' effort to find other remedial strategies such as LIDAR. These highly accurate digital data are used with other digital information to analyze flood hazards and delineate floodplain boundaries.

2. Military Applications

Military applications are possibly classified and are not yet known to be in place, but a notable amount of research is underway in their imaging use. LIDAR's higher resolution offers military personnel the possibility of collecting enough detail to identify targets such as tanks, submarines, aircraft and other warfare threats.

a. Bathymetry

The Airborne LIDAR Bathymetry (ALB) system uses a short green pulse of light to measure the depth of the water based on the amplitude of the bottom return. The water measuring depth varies from 1.5 m down to 60 m, depending on the water clarity, the specific attenuation rate of the water and losses at the air (Abbot et al., 1996). Figure 32 shows a bathymetric LIDAR waveform and can be viewed as three different parts: (1) the water surface return which is the first component, (2) the water volume backscattering which increases until the pulse is entirely within the water and (3) the bottom return which is the last signal that arrives at the sensor. Since LIDAR is a monochromatic system, a combination of LIDAR and passive imaging systems would be more effective for bottom classification and underwater threats detection.

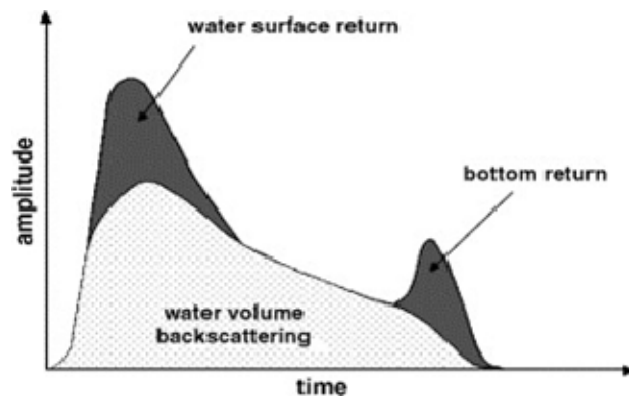


Figure 32. Bathymetric LIDAR waveform (From: Schlagintweit, 1993)

b. Rapid Airborne Mine Clearance System (RAMICS)

RAMICS is one of five developing Airborne weapon systems which will be hosted onboard the MH-60S helicopter. It is a helicopter-borne weapon system that will fire from a gun to neutralize surface and near-surface mines. The gun uses algorithms of targeting and is controlled by a fire-control system. A LIDAR system will be also used by the gun to find the exact location of the mines, target them, provide aiming coordinates to the gun's fire control system and finally fire at the mine, causing immediate mine deactivation. Having this system organic to the fleet, it is possible to

shorten the detection timeline and maximize the helicopter's time on station. Another such system is the Airborne Laser Mine Detection System (ALMDS), which uses the STIL sensor and offers portability and is more effective than the AN/AQS-20X system (Global Security Organization).

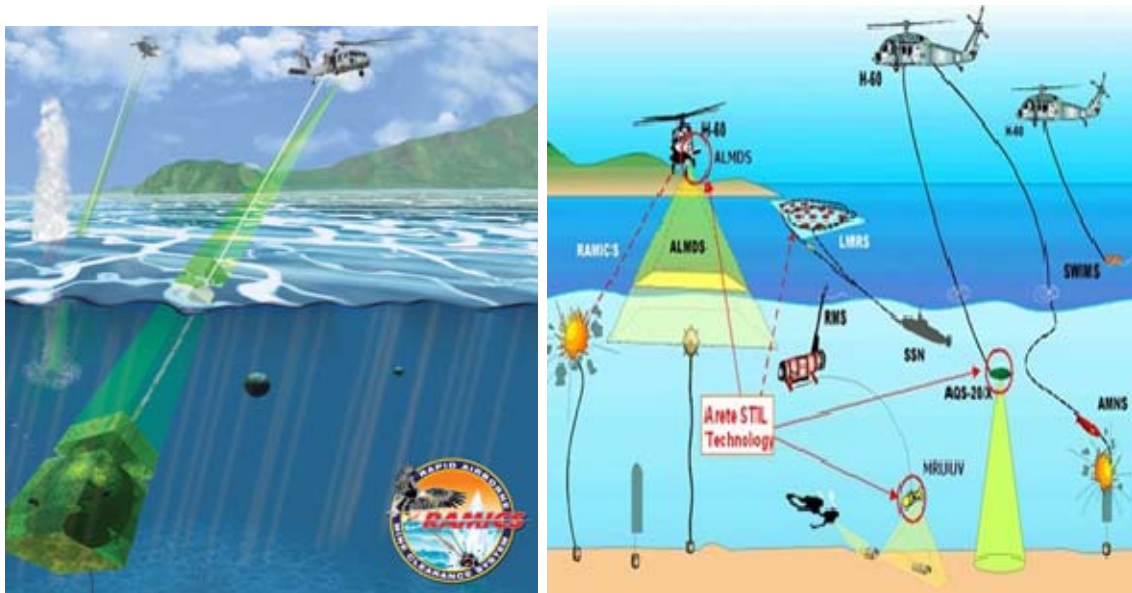


Figure 33. Rapid Airborne Mine Clearance System (RAMICS) and Airborne Laser Mine Detection System (ALMDS) (From: Global Security Organization, 2008)

c. Super-Sensitive Imaging Systems

The need for three-dimensional imaging technology for ballistic missile defense lead in the development of laser-based detection systems that will allow military aircrafts to identify ground vehicles accurately in battle fields and permit robotic vehicles to navigate safely through unfamiliar territory. This technology is built around highly sensitive optical detectors that measure specific amounts of reflected laser light. These systems create 3-D models of scanned objects in real time and due to LIDAR features, this accurate object outline permits interceptor systems to discriminate between re-entry vehicles and spherical decoys, something traditional radar cannot do. 3-D

capable LIDARs can also determine the distance of an object (Kenyon, 2002). The device functions based on the laser pulse, an average, one nanosecond to half a nanosecond long, and its reflected light is imaged by the detector array.

d. LIDAR for Missile Interceptors

The U.S. Army is developing a LIDAR system for next-generation missile interceptors. As part of its advanced LIDAR technology program, Raytheon Company has developed a Range-Doppler-imaging LIDAR sensor to enhance the interceptor's sensing and target discrimination capabilities. This technique uses a laser to scan a target in the same way that conventional radar does. The target's motion can be depicted as an image since range and speed data extracted from the reflected energy of an incoming warhead. This technology offers a huge variety of sensing capabilities based on the Doppler effect for future interceptors against threat countermeasures. The Doppler LIDAR images can be taken at longer ranges than a conventional LIDAR.

All of the above summarizes the broad area of LIDAR operations and applications. The technology is changing day by day as systems are upgraded and new equipment is introduced. In the future, LIDAR is expected to be seen in a large variety of fields of everyday life and soon there will be a learning curve in collecting and using this new tool.

III. PROJECT DESCRIPTION

A. OVERVIEW

Based on Owens and Espinoza's thesis work (Owens and Espinoza, 2007), the experiments in two new areas with different terrain and topology features were applied. Sequoia and Belvoir data were selected as the locations with the most recently collected available LIDAR data. Both sites were utilized for the purpose of identifying trails using these data. After becoming familiarized with Quick Terrain Modeler (QTM) software, data sets were initially loaded on the computer, analyzed and finally divided into training and purpose sub-locations. This dichotomy was important to find training points suitable for the researchers to become comfortable with LIDAR data formatting. Fort Belvoir was the first location and all training points were selected to be from there. During the Belvoir data process, new data from the Sequoia area were simultaneously collected. Belvoir data were recorded during the winter season in leaf off conditions and Sequoia data during the summer season. Although both areas have different species of trees and types of terrain features, the same basic principles were applied to both.

One of the purposes in the experiment was to classify the vegetable area into three categories: i) the bare earth, ii) objects above the bare earth to some height and iii) the remaining cloud of vegetation points above the objects category (Figure 34).

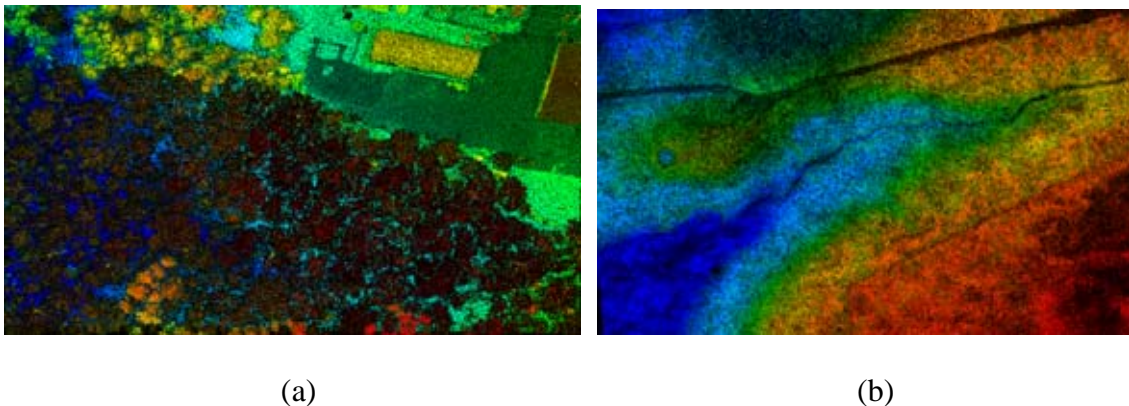


Figure 34. (a) Fort Belvoir original QTM image and (b) bare earth extracted image

Using the bare earth algorithm, the initial data were divided into the above categories. Initially, some useful tools from the QTM software were used to identify possible trails under canopy in forest locations and cropped them to process in a specific way. After making note of the possible trails (Figure 35), ‘control’ areas of the same size were randomly cropped as the trails to be used at a later time for statistical analysis with IDL code. Finally, the check points of ‘target’ and ‘control’ areas were determined that were used during ground truth verification. Points located in the vicinity of a five-meter range from either control or target areas were excluded from the IDL software. Also, a seven-meter buffer zone was established on either side of the trail to eliminate the position errors of selected points due to GPS device, cropping technique, UTM coordinates and GPS accuracy of LIDAR platform during collection.

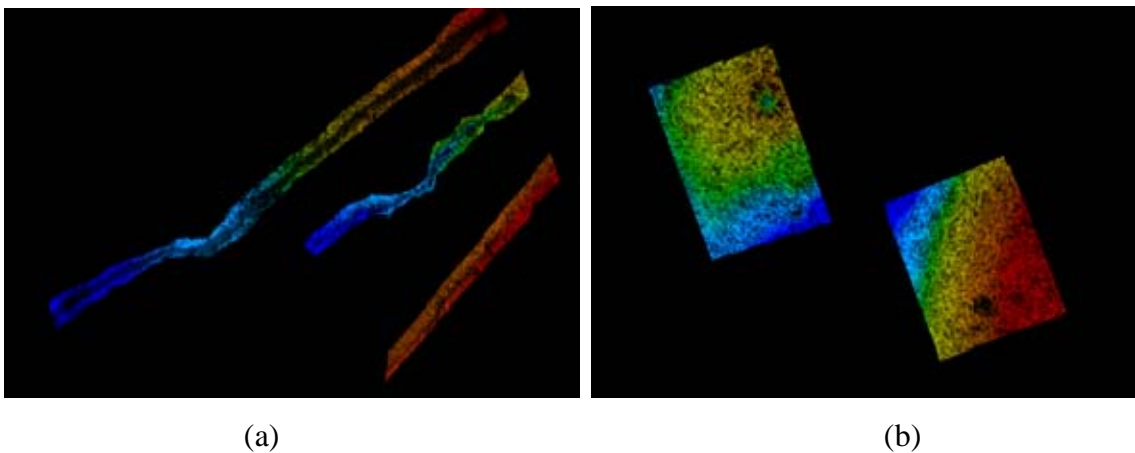


Figure 35. (a) Cropped trail (‘target’ area) and (b) Cropped ‘control’ area

B. LIDAR DATA LOCATIONS

This project deals with two distinct areas with different morphology, topography and biomes. The first location of data sets represents Fort Belvoir in Fairfax County, Virginia (Figure 36), which is a United States military base. The second set of data comes from Sequoia National Park in Southern California (Figure 37). Site descriptions will follow in the next section.

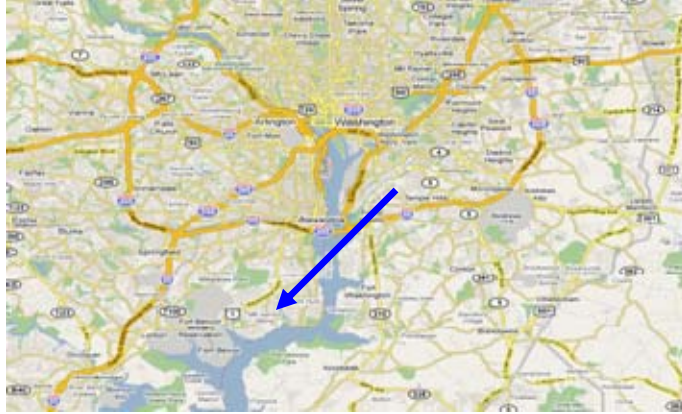


Figure 36. Fort Belvoir in Virginia (From: Google Map)

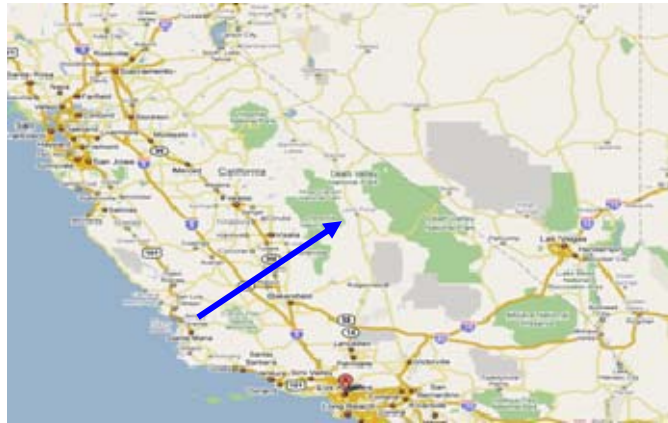


Figure 37. Sequoia National Park in California (From: Google Map)

C. DESCRIPTION OF SELECTED AREAS

In the locations described below, the orientation of the area and some general information relative to geographic characteristics and topography features such as slope as well as canopy and undergrowth composition are supplied.

1. Fort Belvoir

Fort Belvoir base is located about 20 miles southwest of Washington, D.C. It is the home of the United States Army Material Command, Defense Logistics Agency headquarters and elements of ten other Army major commands. The mission of this army installation is to provide both logistical and administrative support to tenant and satellite organizations.

The site is considered to be an urban, flat area with many creeks and small forests. There are different species of trees. For example, there is a mixture of oak mesic and beech mesic trees often located at the tops of hills such as few mixed pine hardwood forests where Virginia pine is dominant (Fort Belvoir).

To cover the entire area (Figure 38), several passes from buckeye flights provided a wide overview from different look angles (Figure 39), conducted over three days. North-South and East-West flights covered portions from the whole area of interest.



Figure 38. Area covered by LIDAR sensor

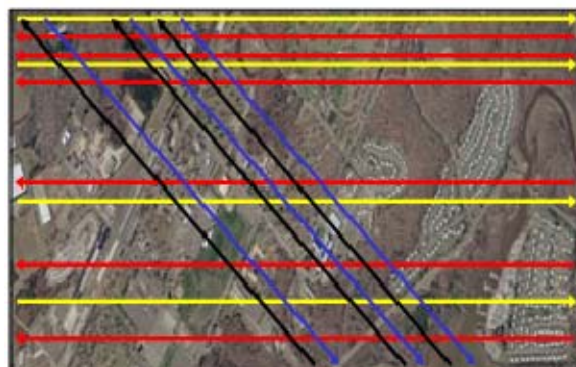


Figure 39. Flight passes

The data were collected using a modified Optech 3100D (Figure 40) on 25-27 March 2007 and some general specifications are found in Table 3. A ground truth site visit was scheduled for August 2008, but was never realized, due to military restrictions. The airborne system was flown at a medium altitudes of 2,500 ft. and recorded a large area, but with relatively low resolution. After the initial flight, the airborne system moved

to lower altitudes to focus on smaller areas (sites 1A and 4B), but with higher resolution data. Both areas have a nominal density of 400 XYZ points per square meter, giving the desired 5 cm surface spacing. In areas with foliage, the density can be much higher than this due to multiple returns per laser pulse. Area 2 was to be collected with nominal point spacing of 30 cm. As most of area 1A and all of area 4 were contained in area 2, the much higher data density was down sampled to 30 cm for this site.



Figure 40. The ALTM 3100EA is the solution for engineering and corridor applications to collect higher altitude missions if demanded

The data contained Buckeye imagery collected by Flight Landata. All nadir imagery was collected on March 25, 2007. The 25 degree off-nadir flights occurred on March 26-27, 2007. For each pass, raw image files and telemetry were provided in the standard Buckeye format. Each area required different data processing. Site 1A is forestry area while site 4B is marshy ground and was mostly covered with water.

Sensor	Optech ALTM 3100
Collection Date	March 2007
Platform	Bell 206 Jet Ranger Helicopter
Operational Altitudes 1	80-3500 m AGL, nominal
Horizontal Accuracy 2	1/5,500 x altitude (m AGL); 1 σ
Elevation Accuracy 2	<5–20 cm; 1 σ *
Effective Laser Repetition Rate	Programmable, 33 – 100 kHz
Range Capture	Up to 4 range measurements, including 1st, 2nd, 3rd, last returns
Intensity Capture	12-bit dynamic range Measurements for all recorded returns, including last return
Scan FOV	Programmable in ± 1 . increments;
Scan Frequency 3	0 to 70 Hz (>70 Hz optional) Programmable in 1 Hz increments
Roll Compensation	$\pm 5^\circ$; more compensation available if FOV reduced Programmable in ± 1 . increments
Position and Orientation System	POS AV 510 OEM Includes embedded BD960 GNSS receiver (GPS and GLONASS)
Data Storage	Ruggedized removable SCSI hard disks
Beam Divergence	Dual divergence: 0.25 mrad (1/e) and 0.8 mrad (1/e) , nominal
Laser Classification	Class IV (US FDA 21 CFR)
Power Requirements	28 V 35 A (peak)
Operating Temperature	Control rack: +10 $^\circ$ to 35 $^\circ$ C to +35 $^\circ$ C (with provided sensor insulating jacket) Sensor head: -10 $^\circ$
Storage Temperature	Control rack: -10 $^\circ$ C to 50 $^\circ$ C Sensor head: 0 $^\circ$ C to 50 $^\circ$ C
Humidity	0-95% non-condensing
Dimensions and Weight	Control rack: 65 cm x 59 cm x 49 cm; 53.2 kg Sensor head: 26 cm x 19 cm x 57 cm; 23.4 kg
Video Camera	Internal video camera (NTSC or PAL)

Table 3. Optech 3100 Specifications (From: Optech, 2008)

The Fort Belvoir area experiences a variety of weather conditions during the year, so any measurements throughout the year will differ from each other due to seasonal changes and natural vegetation growth. Some trails might seem to be the result of naturally draining rivulets down the hillsides.

2. Sequoia National Park

Sequoia National Park is located in the middle of California, approximately 280 nm southeast of San Francisco (Figure 41). It was established in 1890 and is one of the America's oldest National Parks and is considered a national treasure. The park spans 404,051 acres (1,635.14 km²). Elevations rise to nearly 13,000 feet (3,962 m) and the park contains among its natural resources the highest point in the conterminous 48 states. Visitors can find the five largest living giant sequoias in the world, including the General Sherman tree, the largest tree on earth. These sequoias can be 2000-3000 years old. Although they are long-age trees, today only a few trees have survived from the initial sequoia forest. There is a great deal of precipitation and snow to support sequoias and their forest neighbors (White, 2003).



Figure 41. (a) top view from Moro Rock, (b) meadow surrounded with pine trees

The forest consists of several sequoias and other species of redwoods, with an average upper canopy height of 75-80 m and small suppressed trees from 15 to 20 m high. In areas of interest, the canopy closure is about 60 - 70 percent, which is a common closure for this type of forest, while the rest of the park is surrounded by an average upper canopy of 55-60 m. It is considered a dense forest.

Several sites were chosen to set up the measurements, mainly based on trail accessibility (near the main road). Other factors taken into account include the vegetation density and canopy cover, which are very important parameters for this selection and the ongoing analysis. Prior to the visit, more sites had been evaluated but only three were

accessible during the visit (Figure 42). In the tracking area, several dead trees also covered most of trails, making it difficult to walk in the forest. However, many paved trails among sequoia were found that were accessible to everyone.

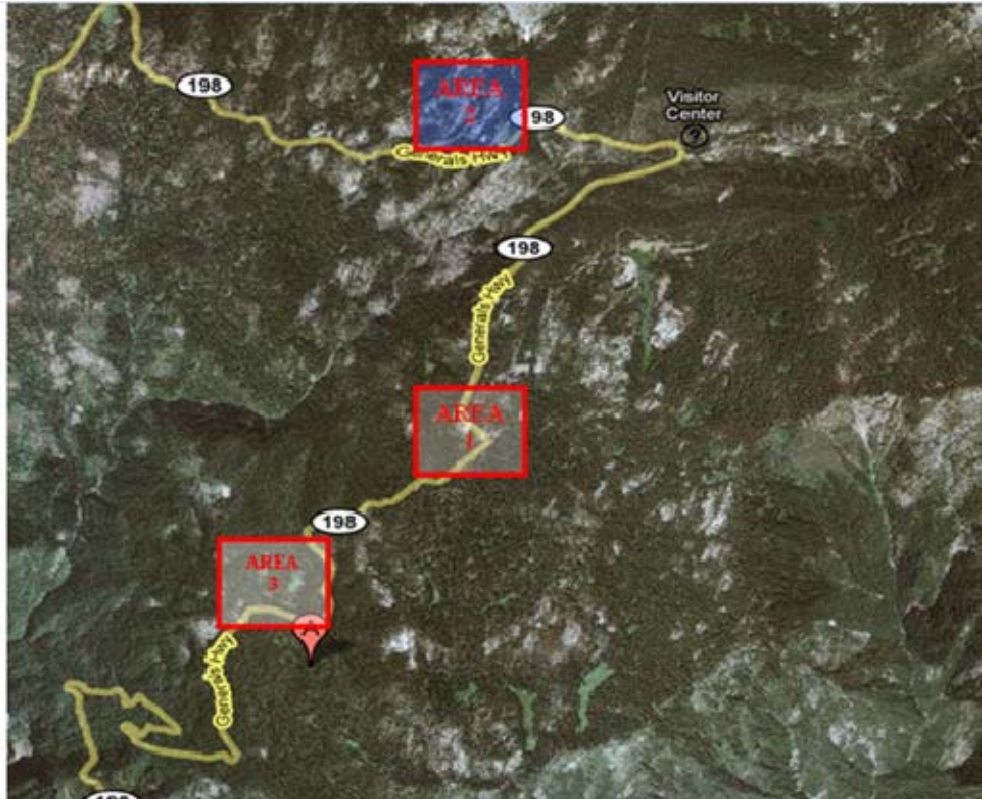


Figure 42. Selected three areas for trail identification

The availability of information at the time of measurements, compared to the availability at the date of collection, remained the same because of the recently recorded data. The size of the entire area recorded by Airborne 1 was almost 100 nm² (Figure 43) and data were taken from a typical flying altitude of 3000 ft AGL. Figure 44 represents the provided flight parameters set on the sensor and the airplane during the experiment.



Figure 43. Area covered by Airborne 1 flight

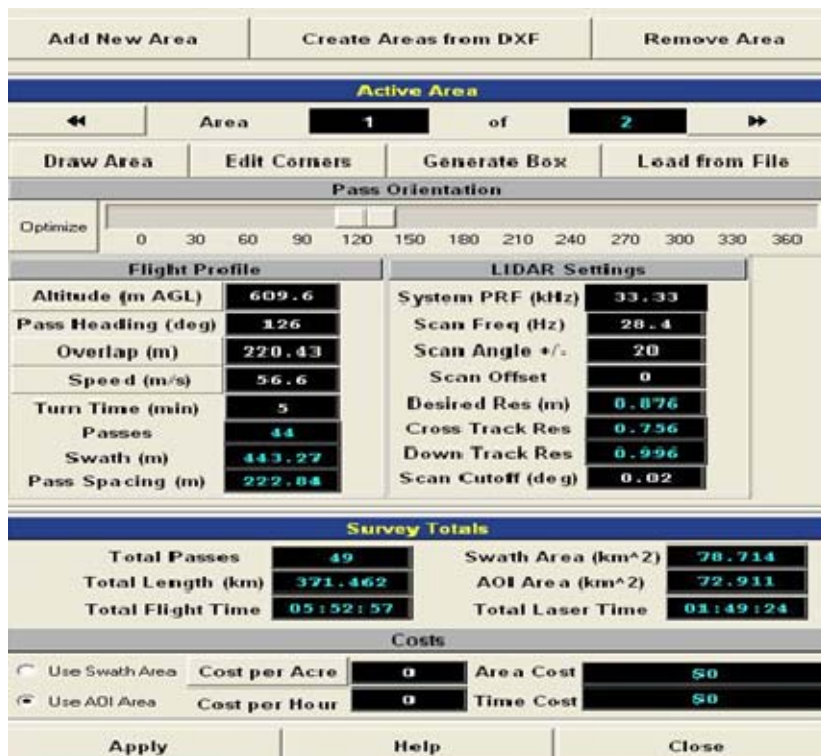


Figure 44. Screen capture of the flight parameters that were used on the captured LIDAR images

C. FIELD EQUIPMENT

Table 4 identifies equipment utilized during ground truth verification site visits.

FIELD EQUIPMENT	
Equipment	Description
Garmin GPSMAP 60CSX	Hand-held GPS receiver used to verify target and control points
Antcom L1 TNC female 5" ground plane, 5/8" mount, 35db	GPS External Antenna (Backpack Mounted) for increased GPS accuracy and signal acquisition under canopy.
Kodak 10.0MP Digital Camera - Black (Z1085)	Digital camera used to capture overhead cover and trail characteristics
Galileo Zoom Binoculars - 8-24x50mm	Locating the most distant trails other general use.
Western Digital Passport External Hard Drives with 250 GB of Memory	Transfer data during site visits
Portable laptop	Software Garmin installed, QTM software installed

Table 4. Field Equipment

IV. OBSERVATIONS

A. TRAIL AND ROAD CLASSIFICATION

Various definitions are given for trails (Figure 45). Generally, a trail is any surface designed and managed to accommodate use on that surface. From a civilian aspect, according to Interagency Trail Data Standards (ITDS) Version 2, the Interagency Trail Fundamentals suggests four fundamental concepts that are cornerstones of effective trail planning and management:

- Trail Type
- Trail Class
- Managed Use
- Designed Use



Figure 45. Trails samples in Sequoia National Park and Fort Belvoir

The above categories provide the means to design and manage existing trails and how to use them (nps.gov, 2004).

Trail Type is assigned per each trail and helps managers to indentify trails based on design parameters, management needs and the cost of managing any trail for a particular use. It is subdivided into three fundamental categories: i) Standard/Terra Trail, ii) Snow Trail and iii) Water Trail.

Trail Class provides chronological classification of trail development:

- Trail Class 1: Minimal/Undeveloped Trail
- Trail Class 2: Simple/Minor Development Trail

- Trail Class 3: Developed/Improved Trail
- Trail Class 4: Highly Developed Trail
- Trail Class 5: Fully Developed Trail

Each Trail Class is defined in respect to accessibility to the public, traffic flow, obstacles, and constructed feature. When Trail Classes are applied, the one that most closely matches the managed objective of the trail is chosen.

Managed Use indicates a management decision or goal to accommodate a specified type of trail use. Trail Class and Managed Use are mutually connected, and one cannot be determined without consideration of the other.

Designed Use is unique for each trail and shows the intended use that controls the desired geometric design of the trail, and determines the subsequent maintenance parameters for the trail. The Designed Use determines the technical specifications for the design, construction and maintenance of the trail or trail segment.

From a military point of view, only a route classification determines what type of vehicle and traffic load a specific portion of a route can handle. The route-classification formula consists of the following route features (Espinoza, 2007, p. 34).

- Route width, in meters
- Route type (based on ability to withstand weather)
- Lowest military load classification (MLC)
- Lowest overhead clearance, in meters
- Obstructions to traffic flow (OB), if applicable
- Special conditions, such as snow blockage (T) or flooding (W)

For trails and roads classification, the most visible and easy to measure parameter for the identification of trails with QTM is the width of the trail. Therefore, each trail that shows up in the LIDAR data with a certain width can be considered as a potential trail. However, further analysis of other characteristics (height profile and intensity) of the data will confirm or deny the existence of the trail. The width of the trail is a significant factor that makes it possible to estimate the designed use of the trail, and furthermore, the condition of the trail shows its accessibility. In most U.S. military maps, the lane width of

trails is less than 1.5 m (Espinoza, 2007, pp. 34-35), while Table 5 illustrates the various measurements applicable to road width according to STANAG 2174 for military routes (Global Security Organization).

Flow Possibilities	Road/Route Widths
Limited Access	Up to 3.5 m (11'6") incl.
Single Lane	Between 3.5 m (11'6") and 5.50 m (18 ft.) incl.
Single Flow	Between 5.50 m (18 ft.) and 7.30 m (24 ft.) incl.
Double Flow	Over 7.30 m (24 ft.)

Table 5. Road classification according to the number of lanes

Figure 46 shows terms used to designate road features and components. This is similar to the description of a trail. Each trail consists of the traveled way (the main “body” of the trail designed for foot traffic) and the shoulder at either side of trail. In the case of paved trails during this experiment, one measurement was taken from the width of the traveled way and another measurement included the width of the shoulder (Figure 47). For unpaved trails, the extreme width was taken from one side of the depression to the opposite side to provide the visible indication of the trail to the analyst (Figure 48).

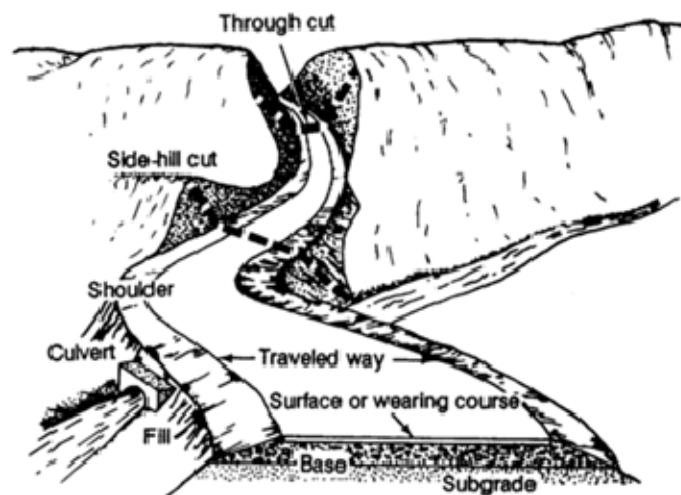


Figure 46. Road nomenclature

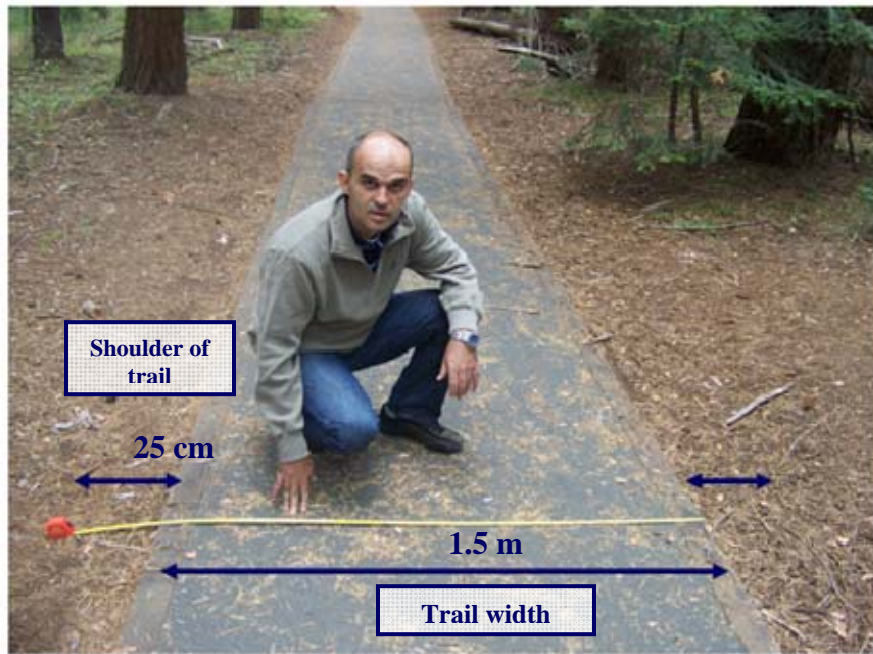


Figure 47. Paved trail in Sequoia National Park



Figure 48. Unpaved trail in Sequoia National Park

B. RESEARCH METHODOLOGY

As mentioned earlier, each area was subdivided into control and target areas and a number of these were randomly selected as samples for ground truth verification. Although 50 points are recommended for ground truthing of small areas, the software generator used randomly selected only approximately 20 points for each area to be verified (Figure 49). This may have occurred because most of the trails recognized in the data were shorten in length. The number of control points selected for each area was approximately two-thirds the number of target points.

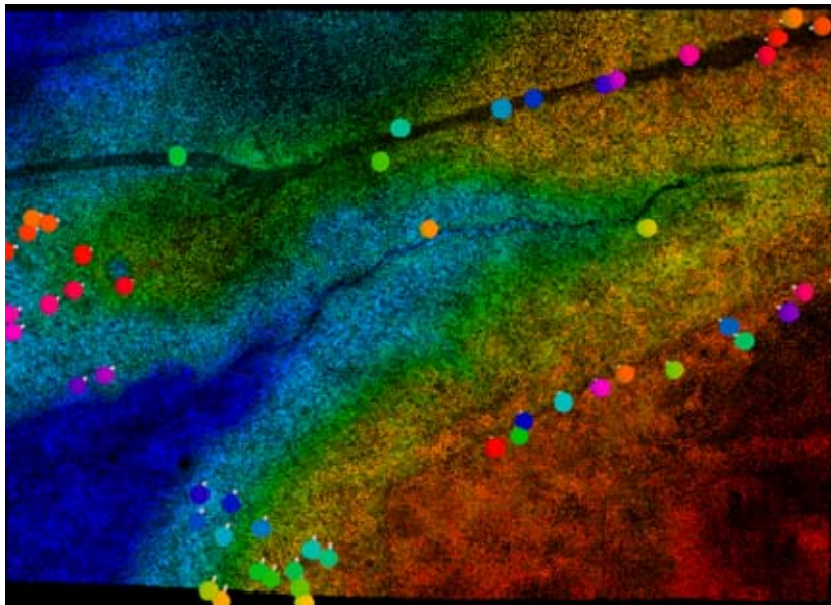


Figure 49. Randomly generated points for both target and control areas.

To extract the accuracy of the measurements, all measurements taken are plotted in tables in Appendix B. Based on Airborne 1 accuracy tables, the standards of NMAS – VMAS of typical resolution (Airborne 1, 2008) was adopted. This experiment depends on a 90 % confidence, which implies that the points measured inside the circle with 0.5 m radius from the selected point (center), were defined as trails and used for the trails accuracy calculations (Figure 50). A numerical adjustment of 20% on the radius of 0.5 m occurred on the above standard for the Sequoia area. Consequently, the limit of 0.5 m

increased to 0.6 m, which is justified from the morphology/topography of that location and the difficulty that LIDAR sensors have in measuring the data on hillsides precisely. Chapter V provides more details in the analysis.

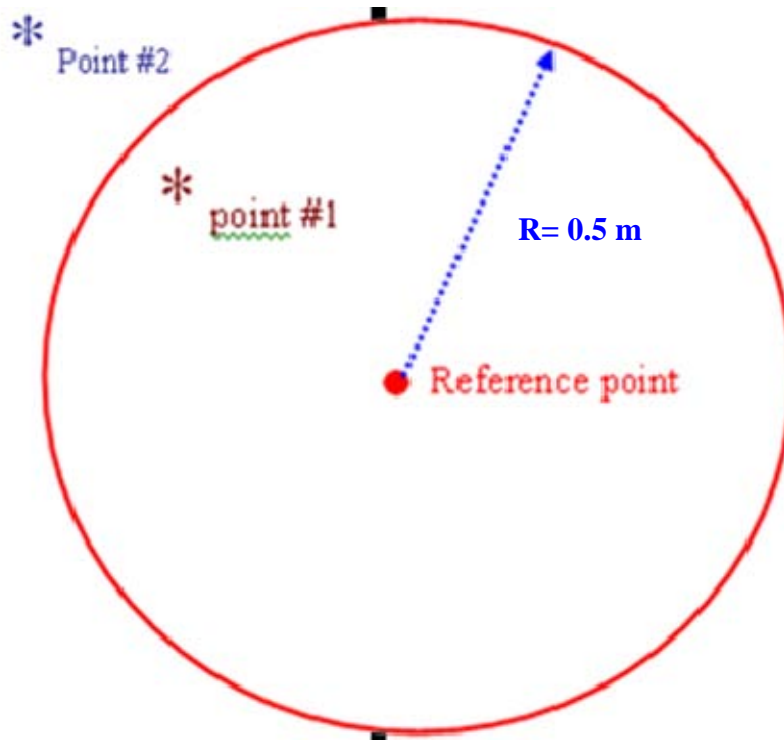


Figure 50. Point #1 is considered to be inside the range of 50 cm radius cycle, while Point #2 is outside. Point #2 was not characterized as a successful result due to its distance from the reference point.

Remarkably, all other points plotted outside the circle do not suggest that the LIDAR sensor and QTM software totally failed. As mentioned in Chapter II, errors such as GPS Positioning and IMU orientation errors can completely justify that deviation. Many other functions were also used to define the accuracy with mathematical precision of all the points on trails. As seen in the sample table (Table 6), the mean of the real values is mostly calculated to show the sign and the value of the result number, indicating where the points tend to be forward or backward along the direction of the trail path. Figure 51 represents a pattern of two trails and four sample points (two for each one). It

should be mentioned that no relation exists between the arrows ending direction with the North axis. As explained below, the arrows indicate the hiker's footpath from alongside the trail.

AREA		
Points		
Target Points	Measured distance from point (Real-Absolute values) (m)	
1	0.40	0.40
2	-0.30	0.30
3	0.70	0.70
4	-0.20	0.20
Mean of the real values (m)	0.15	
Mean of the absolute values (m)		0.40
RMS (m)	0.441588043	
Average of points inside the trail	3 of 4 = 75.00 %	

Table 6. Template, similar to those created from the experiment, used to analyze the results

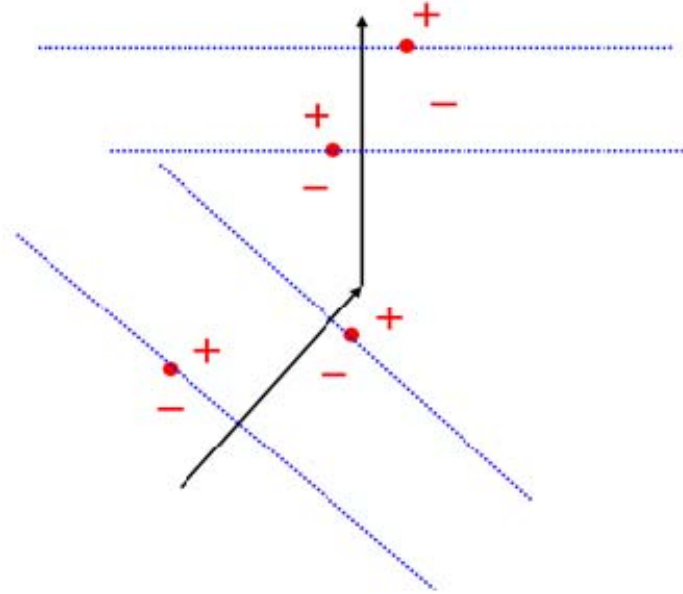


Figure 51. Red dots represent the points (targets and controls) and the arrows show the direction of the trail. Blue dashed lines are perpendicular to the mean direction axis of the trail and pass from the point. The signs + or – represent the distance that is forward or backward (respectively) of the point and have a positive or negative number.

The mean of the absolute values is very significant because that result gives a representative sample of the dispersion of the true points during measurements. It refers to the average and the mathematical success of the experiment. Finally, the Root Mean Square (RMS) is the statistical measure of the magnitude of the deviation between points from LIDAR and points from the GPS unit. The grey shading (Table 6) indicates the points that exceed the limit of 0.6 m and are excluded from the ground truth data identification.

C. DATA COLLECTION TOOLS AND PROCEDURES

During area observations and data analysis many considerable characteristics were analyzed, not only of the QTM software, but also from the areas where the measurements took place. Areas that had sunk below specific locations often appeared to be trails or roads, but were not. The overhead panchromatic imagery, either from the LIDAR sensor or Google mapping, initially provides the image of a flat area on the

ground. With further examination, using the “rescale model height” and the “examine height profile” tools from QTM it is now easy to recognize the existence of a natural depression (Figure 52).

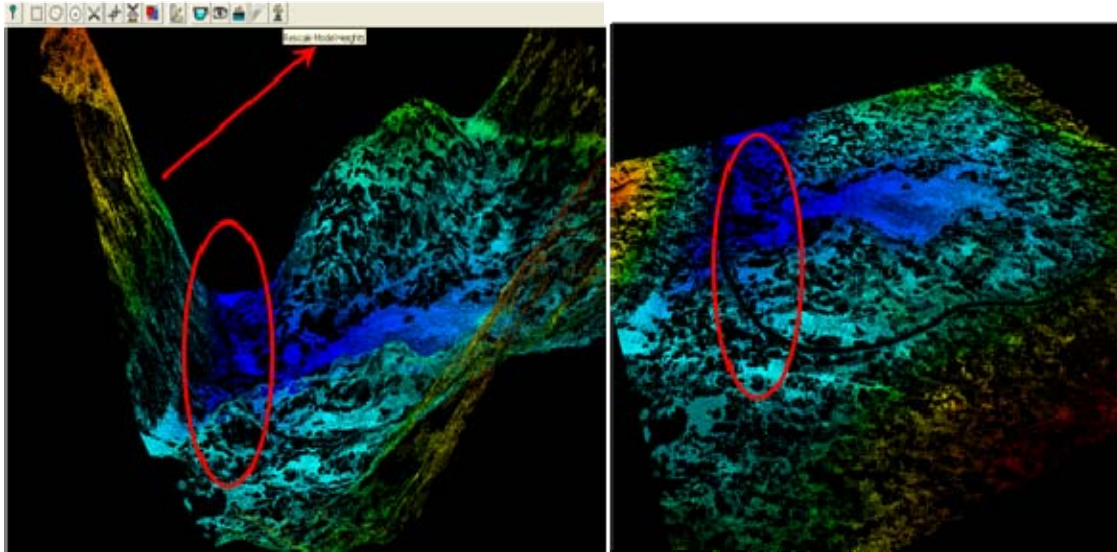


Figure 52. Rescale model height tool: (a) exaggerated top view showing the depression in Sequoia National Park (b) default values for the depression in that area.

As already mentioned in the Espinoza and Owens thesis, the height profile tool across a depression provides a remarkable solution to identify whether or not a feature is man-made or natural. The “V-shape” of the height profile is a good indication for distinguishing between trails or roads and natural drainage areas.

Another useful visualization option provided by QTM software is the intensity enhancement. By checking the import intensity box during the import XYZ model process, it is then possible to examine the intensity profile across a line on a specific location. The intensity profile is primarily used to classify the texture of the target. A representative example in the following Figures 53-56 shows the intensity profile across the creek in Fort Belvoir, which is depicted as a flat depression line.

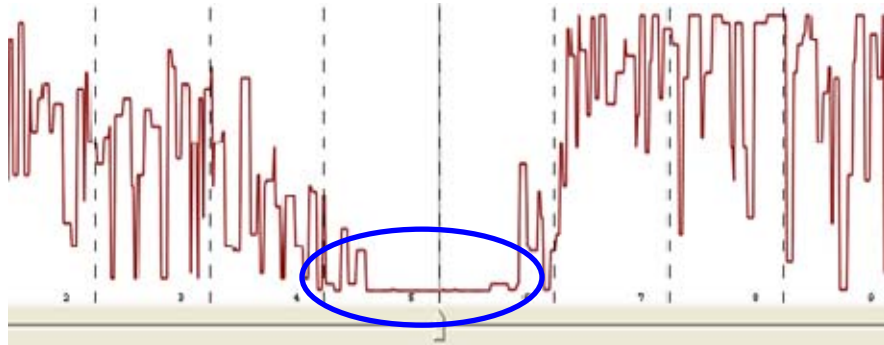
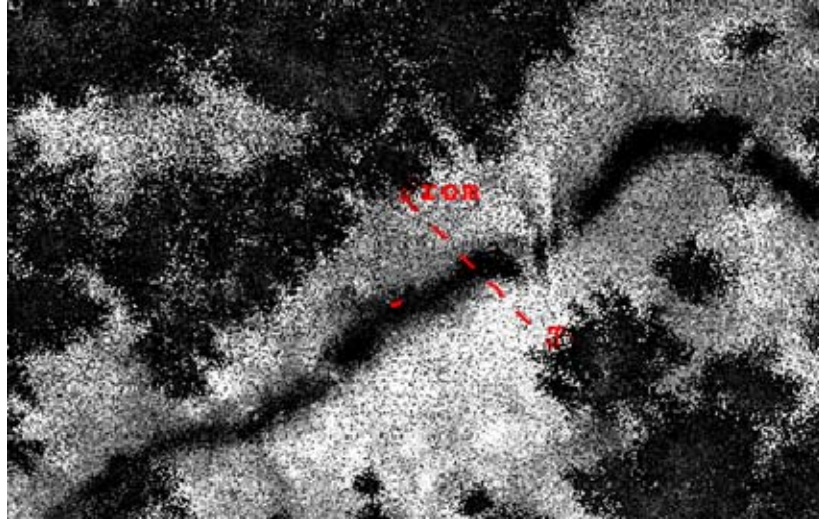


Figure 53. Creek with a width of two meters width in Fort Belvoir measured by QTM and its corresponding intensity profile

Paved roads or busy trails can be identified with more accuracy since the intensity profile detects any irregularity of the ground. On the other hand, it is not obvious if it is a trail or just the result of a natural drainage rivulet. Unpaved trails have almost the same features as a paved trail, with the only difference of the vegetation that covers the trail and also a fluctuation in the width of the trail that results in different intensity profiles. The fluctuation on the intensity profile diagram along trails confirms the existence of an asphalt paved trail (Figure 54) and wooden paved trail (Figure 55).

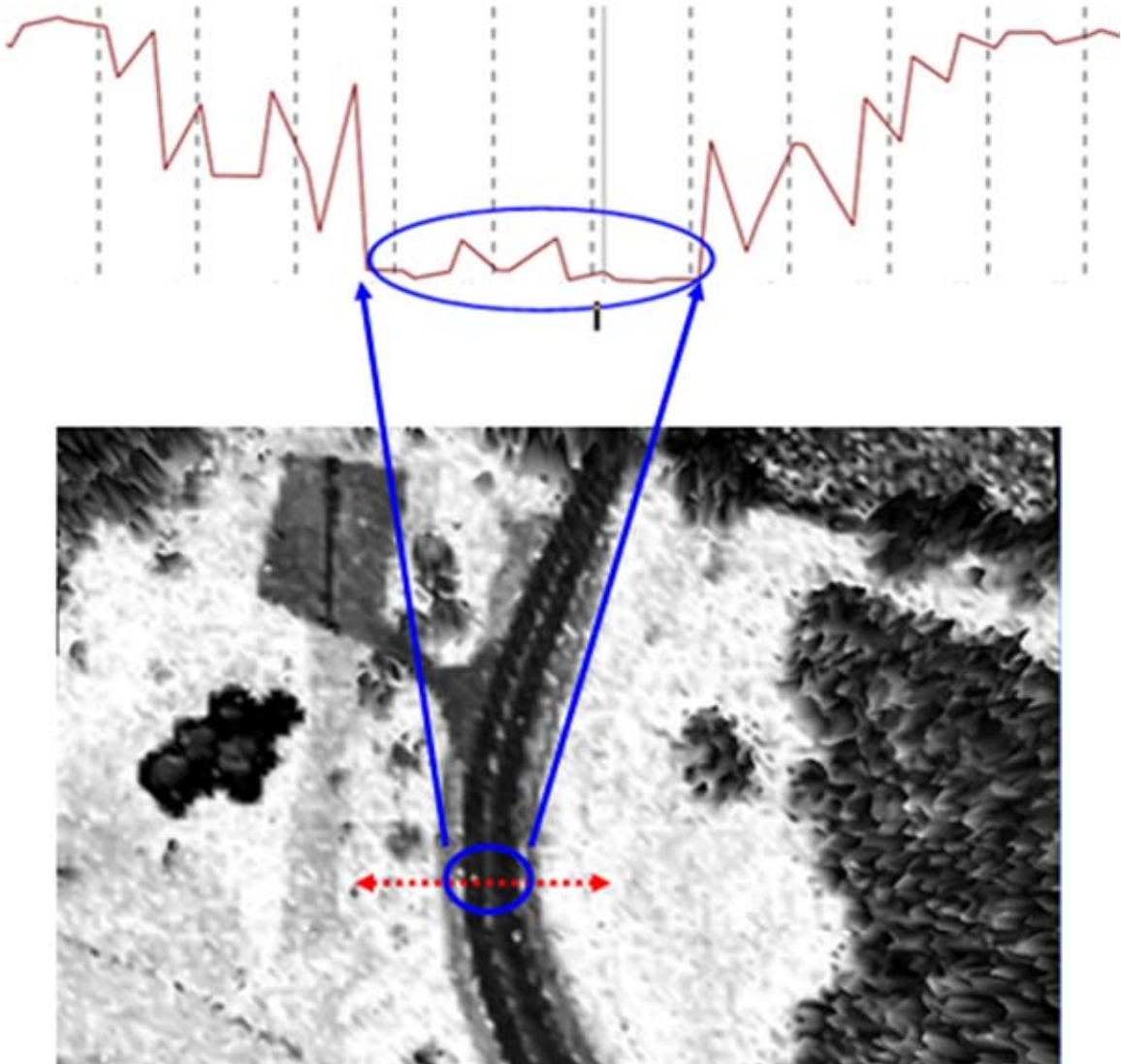


Figure 54. The rough fluctuations on the bottom of the “well” along the intensity profile correspond to the *asphalt* paved trail

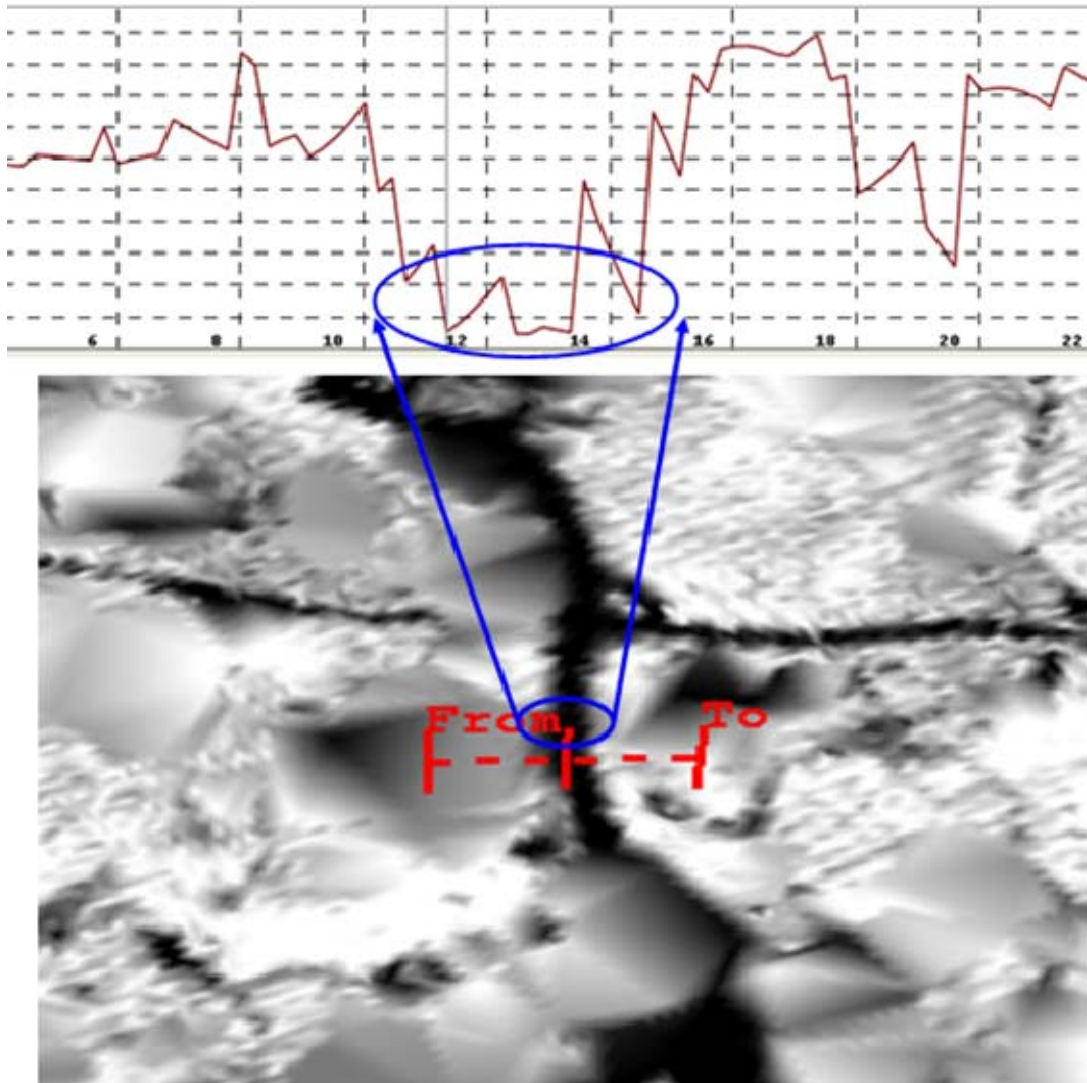


Figure 55. The rough fluctuations on the bottom of the “well” along the intensity profile correspond to the *wooden* paved trail

V. ANALYSIS

A. FORT BELVOIR

Fort Belvoir was the first site analyzed using techniques, described in Chapter IV. The data were collected on March 25-27, 2007. The sensor was mounted onboard a rotary wing aircraft. This collection method provided multiple look angles, increasing the probability of recording more returns from the surface below. The area consisted of eight sites, as described in Chapter III.

Unfortunately, Fort Belvoir is a military restricted area and it is not possible to gain access. However, it was possible to collect some information about this area from the internet. The entire site was recently converted from a forestry area into an almost urban area. There is a small possibility to detect trails among houses, especially since one third of the area was flooded (area 4B in Figure 38). Data were collected during leaf-off conditions, although evergreen trees were present. From the available three sites, eight smaller areas were selected that could contain potential trails. From each area, the possible trails were cropped and called target areas. The total size of the added target areas was used to create another randomly selected area of equal size, that was denoted as control area. All points were selected using a minimum distance rule of 5 m from each location. The sample sizes were randomly selected and differ from one site to another depending on the size of the area.

From the larger area No 2, three trails were manually selected and a total number of 40 target points and 40 points randomly selected points for ground truth. Of the rest of the areas, an average of 10 points was used for each control and target areas (Table 7).

FORT BELVOIR POINTS AND SIZES				
Type Areas	Target Size(m ²)	Target Points	Control Size (m ²)	Control Points
Sub Area-1A_1	731	11	740	7
Sub Area-1A_2	410	8	410	5
Sub Area-1A_3	2688	34	2700	26
Sub Area-1A_4	838	12	840	8
Sub Area-1A_30	596	8	600	5
Sub Area-1A_31	541	15	540	10
Sub Area-1A_32	446	20	450	16
Sub Area-2_2	10714	60	10720	40

Table 7. Fort Belvoir Sub-areas size and its corresponding target and control points

An advantage of this area was that almost vertical pictures were taken along the flight lines at the same time as the airborne LIDAR system recorded the underneath surface. This made it possible to compare the real picture with the LIDAR data of the same area and recognize trails in areas where the ground was visible among the trees.

It was a challenge to develop methods to recognize creeks with LIDAR. Some visible creeks recognized in the images were deliberately selected to prove that with the LIDAR system it might be possible to distinguish a creek from a trail. The LIDAR data had very good resolution that made it easier to detect any type of trail on the ground. The height and intensity profiles were very useful tools that supply an accurate prediction of the type of the trail. With the intensity profile, it was possible to predict the presence of flowing water in some creeks based on the intensity values (intensity falls when the laser beam is reflected on a water surface) (Figure 56).

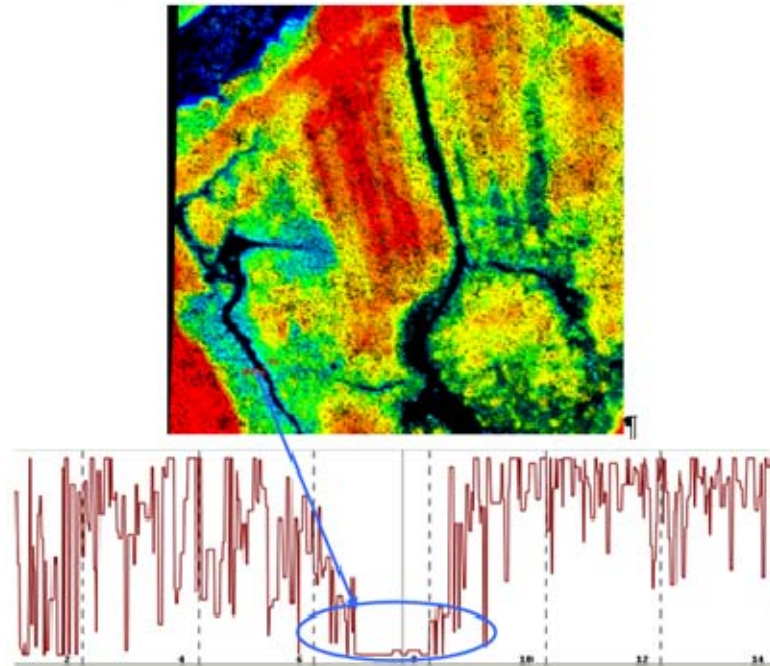


Figure 56. Area 4B and its corresponding height profile below

The height profile of any trail indicates if it is a soil depression or natural drainage. Generally, man made trails have a start and an end point between two human facilities, which are additional features that someone can use to estimate human traffic and the accessibility of the trail. If a trail's end point was at a river, they were considered to be creeks. Trails not connected to roads or other human facilities were thought to not actually be trails.

Trails not visible in the images were considered to be covered by vegetation (recognized during the analysis of the data using QTM software). This meant that they might be natural drainages or an unused human trail that had overgrown low vegetation. Other areas with linear depressions that caused them to appear as trails were visible on the surface model. Using the QTM software, the object file by itself can also provide visual queues to the existence of trails through linear gaps in the model where there is no vegetation at the specified AGL or below.

Finally, some lodging 3-D data were provided from the area and some LIDAR data from small ports in the river that show the accuracy and the resolution of the data provided from that area. Also, it is possible to detect some high voltages wires. It is remarkable that this area is offered for multiple type LIDAR data analysis (Figure 57).

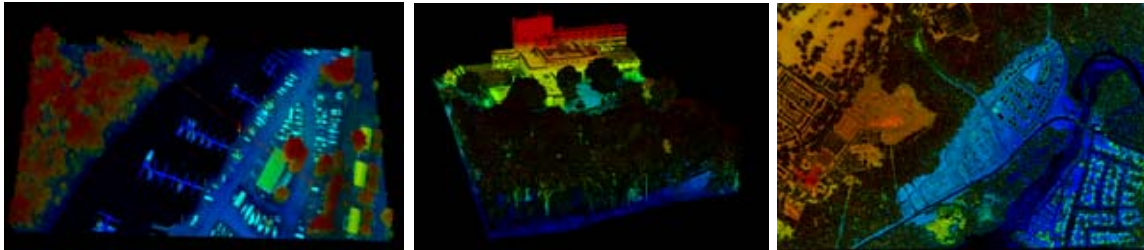


Figure 57. High resolution of Fort Belvoir Data illustrates the three images

B. SEQUOIA NATIONAL PARK

Sequoia data were collected in August 2008 from Airborne 1 Company, just one month before the visit. The system's accuracy is about 50 cm horizontally and 50 cm vertically for flat surface. However, unlike the Fort Belvoir site, Sequoia is mountainous area and certain factors were taken into account such as the slope of the mountains and the height of the trees. As mentioned in Chapter II, the height of the tall trees can be underestimated when near other shorter trees. These factors reduce the overall accuracy, so it was necessary to increase the position error. For Sequoia data, a 60 cm horizontal and 60 cm vertical accuracy were used.

The season that the data were recorded did not affect the results of these experiments because these trees are evergreen. However, some seasonal trails were created into some drainage trails due to the summer drought and were used by people as trails during the summer. The area of interest included some of the world's larger sequoias. The network trail was in a tourist area among sequoia trees, which meant that most of the trails were paved. The paved trails are easier to recognize with Quick Terrain Modeler because they give a lower intensity profile. The unpaved trails were not identifiable using the intensity profile of these data. Only the height profile could be determined, but it was difficult to detect unpaved trails during data analysis (Figure 58).

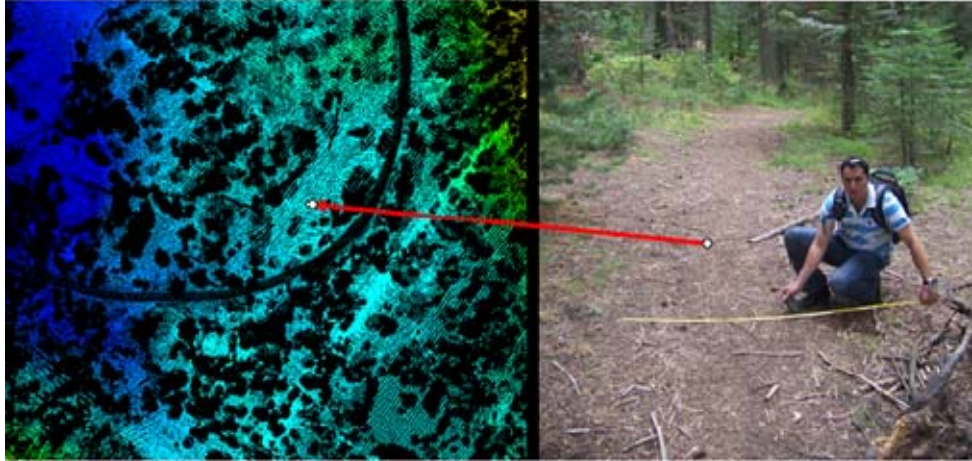


Figure 58. Unpaved trails not identified with LIDAR data

The target points of paved trails were easily recognized because it was easy to locate the paved trails using a map available from the Sequoia National Park's official site. Although the ground truth verification of control points were done, this research demonstrates mostly the verification of the existing paved trails identified in the data. Control points represent a subtotal of the entire area, while the target points are extracted from all the detected trails in the area. Also, in this research, trails plotted in the map were identified to evaluate LIDAR system as a mapping tool.

It can be verified that the resolution of the data was the main factor that did not permit the identification of unpaved trails. Unpaved trails, with a width less than 1.5 meters, were not displayed during the analysis of the data. Using these data, only paved trails were identified during this visit. To prove that, the inverse procedure was used. During this visit, some unpaved trails on a map with the same width (1.5 m) were plotted. Afterwards, the data analysis was repeated and attempts were made to identify them, but it was impossible. For this kind of analysis, much higher resolution data are required and more points must be collected from the ground. An empirical estimation of the resolution of surface data from Sequoia gives 0.5 points per square meter. This is much lower than the required four points per square meter necessary for this kind of analysis. The corresponding resolution of Fort Belvoir data is about 400 points per square meter, resulting in a much better analysis (Figure 59). During this visit, the forest was clear from

low vegetation and branches due to maintenance work. For that reason, someone would expect ground returns of LIDAR with better accuracy and accurate determination of bald earth.

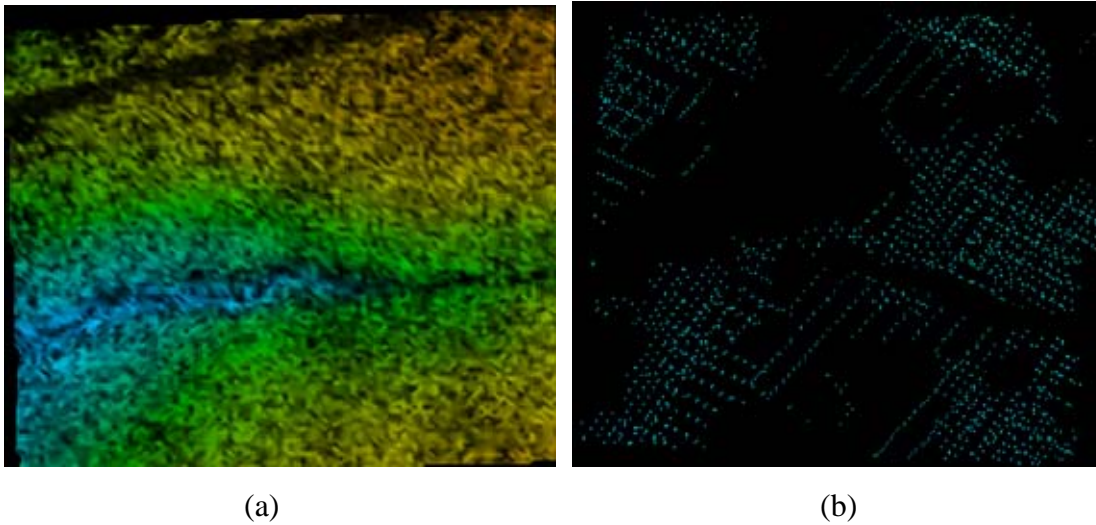


Figure 59. The resolution features from (a) Fort Belvoir and (b) Sequoia National Park

From the original area, three smaller areas were selected with differences in topology and canopy density to evaluate the poke through the capability of LIDAR. The three areas selected for Sequoia National Park consisted of 66 target and 47 control points (Table 8). Due to the slope of the area, points that were falling within six meters of each other were removed from the area. Thus, points falling within 60 cm of each side were considered to be in the trail.

SEQUOIA POINTS AND SIZES				
Type Areas	Target Size(m ²)	Target points	Control (m ²)	Control points
Sub Area-1	1922	32	1900	19
Sub Area-2	5990	22	6000	17
Sub Area-3	2102	12	2100	11

Table 8. Sequoia Sub-areas size and its corresponding target and control points

Also, in the IDL code that randomly generated target and control points, a limitation to exclude points falling within 5 m of each other was inserted. The statistical analysis for Sequoia National Park resulted in a trail accuracy of 83.60% and control accuracy of 86.0% (as shown in Table 9). This accuracy is satisfied for the quality of the data and it turns out that it should be higher for paved trails. All the trails detected during the LIDAR data analysis were successfully located and the accuracy decreased since some points were identified in longer distance than the predetermined system’s accuracy of 60 cm. Thus, all these points classified as no trail should be considered as trails. Therefore, it can be concluded that the overall accuracy for paved trails is close to 100%. On the other hand, in the control areas, some points are classified as trail not showing in the LIDAR surface model. The points misclassified as “non trail” were from Site 3. These points were identified in an area that includes some unpaved trails. The control areas were deliberately not evaluated since it was obvious that many trails were not visible during the analysis of the data. This situation exhibits the need for better resolution and possibly the need for pre-visit inspection of the area to take note of some features of interest.

Sequoia National Park									
LIDAR vs. MANUAL									
Target points						Control points			
AREAS	Total Numbers	Mean of the real values (m)	Mean of the absolute values (m)	RMS (m)	Average of points inside the trail	Total Numbers	Mean of the absolute values (m)	RMS (m)	Average of points inside the trail
Sub-Area 1	32	0.06	0.41	0.467	81,25%	19	0.35	0.399	82,21%
Sub-Area 2	22	-0.05	0.36	0.418	86,36%	17	0.35	0.383	94,12%
Sub-Area 3	12	0.26	0.41	0.506	83,33%	11	0.44	0.461	81,81%
TOTAL	66					47			
AVERAGE		0.090	0.393	0.463	0.836		0.380	0.414	0.860

Table 9. Total results from Sequoia Measurements

THIS PAGE INTENTIONALLY LEFT BLANK

VI. SUMMARY AND CONCLUSIONS

A. SUMMARY

The overall results of this experiment were excellent for the quality of Fort Belvoir data and encouraging for Sequoia data. Also, this study demonstrates the importance of ground truth validation of data to ensure the LIDAR data meets the high accuracy requirements. This contributes to the development of new LIDAR technology and the evolution of new methods for recorded data dependent on the special features of the area of interest. There is an interactive relationship between the researchers that develop the system, the people that fly over a specific area to record the data and the people that make the ground truth. Without the ground truth verification, the accuracy of the system for a specific job cannot be evaluated. The resolution of the collected data should meet the requirements of the people that will use these data. Therefore, the specifications and parameters of the data should be determined by the end user. It is necessary to point out that none of the data were originally collected for the purpose of identifying trails under tree canopies. The decision to identify trails under canopy belongs to the authors of this study. On the other hand, the topography of Fort Belvoir data shows that the data could be mostly used for urban and coastal applications.

Fort Belvoir LIDAR data were more accurate, and supported by complementary information such as images, reference points and geodetic points, that were useful tools for analysis. Also, it was a much easier process analyzing these data to distinguish a trail from a creek or a ground depression. Although data were collected during leaf-off conditions, some areas were covered with evergreen trees. However, this detail did not affect the final result. The authors are confident that if it were possible to visit the area, the ground truth results would be excellent, due to the large number of ground returns and the fact that most of the trails were easily detected even if trail sizes were less than 1.5 m wide. All the detected trails were unpaved and mostly used to connect human facilities.

By comparison to the Fort Belvoir data, the relatively poor spatial point density of Sequoia National Park gave little information of the existing trail network. Only the

paved trails could be recognized. The Sequoia LIDAR data lacked the complementary spectral imagery which was available for Fort Belvoir. This made it difficult to recognize unpaved trails on the ground even in open areas with no trees. Thus, although the control areas were evaluated, it was certain that many trails were not recognizable due to the nature of the data. Furthermore, two researchers with no previous experience conducted the research and data analysis.

The format of LIDAR data contained only discrete returns and did not contain waveform data, which are particularly important to model and predict the texture of return points. Also, no auto-recognition algorithms were attainable and all trails were recognized manually. It is worth mentioning that in forestry applications, full waveform analysis is of significant advantage as it improves the ability to analyze multiple targets with a single laser pulse. With appropriate post processing of the digitized echo waveform, the analysis of the vertical structure of vegetation and the discrimination of vegetation against the ground can be improved upon with respect to conventional systems.

B. CONCLUSION

In this study, it was found that LIDAR is a very promising system that has evolved very quickly. In comparison with previous studies with similar results, it is amazing how fast the accuracy and resolution of the LIDAR system has improved in the past decade. Ten years ago, the pulse rate was about 10,000 pulses per minute, and currently, some systems reach an amount of 250,000 pulses per minute. All the experiments that take place in forestry areas exhibit the same results regarding the specific features that have to be developed in the future. It is obvious that small footprint LIDAR systems have the potential to estimate the forest structure and map the area. A small footprint, multiple-return LIDAR sensor is necessary to predict the Digital Elevation Model. At least four points per square meter are the minimum requirements to identify 1.5 m wide trails. The development of new sensors with higher accuracy, higher pulse rate and with rotational scanner can provide an ideal input for bald earth analysis and hidden trail extraction under tree canopies.

LIDAR tends to be a reliable and cost effective sensor for forestry applications. The estimation of forest volume and biomass and the automatic identification of human facilities and terrain features under tree canopies can further increase LIDAR utility in forestry areas. This allows managers to design human facilities in forests, recreational areas and trail network that can offer unique opportunities to visitors.

THIS PAGE INTENTIONALLY LEFT BLANK

APPENDIX A. FORESTRY DATA PROCESS USING QTM TOOLS

Chapter II made a short reference to the most important steps of the process followed to extract roads or trails under tree canopy. QTM software is a 3-D modeling package developed at the Johns Hopkins University Applied Physics Laboratory (APL) to facilitate real-time manipulation of large amounts of complex 3-D data. It provides many useful tools in processing forestry LIDAR data.

A. BARE EARTH EXTRACTION

The initial process was made with bare earth algorithm.

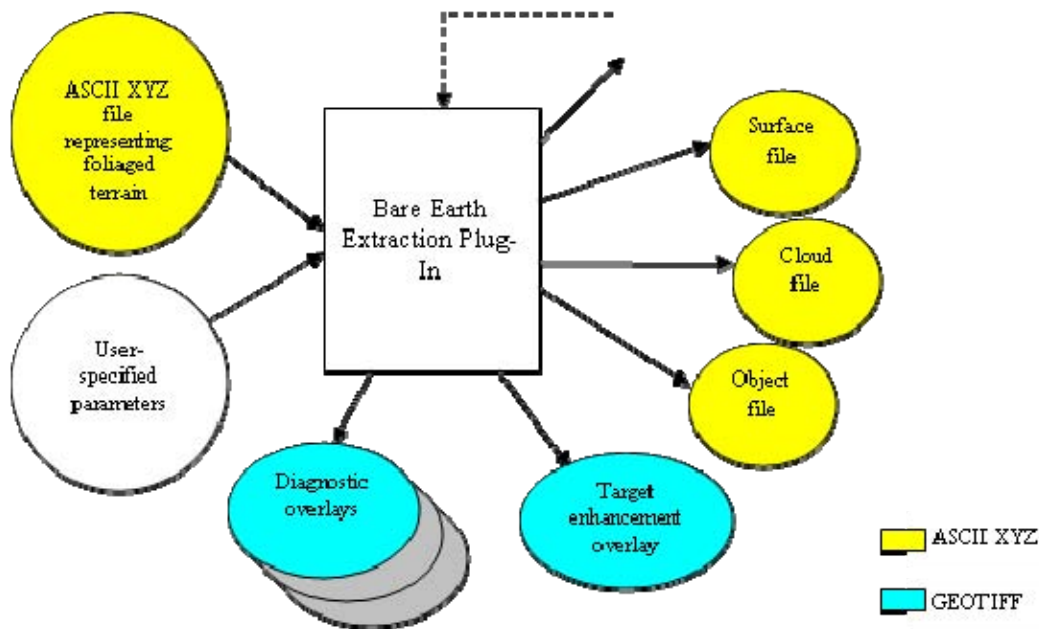


Diagram Showing Inputs and Outputs of Bare Earth Extraction Plug-In

It is a digital elevation model processing utility designed to help the user extract the man-made structures under a tree canopy. The data should be in ASCII XYZ format; otherwise, it needs to be exported into that format. Fort Belvoir and Sequoia data were initially in LAS format and had to be converted to XYZ. The output files of bare-earth extraction are also in XYZ format, but are classified into three major categories: surface, object and cloud. Upon completion, these extracted data are saved into qtt/qtc format.

More detailed Point Clouds (.qtc) are good for visualizing the data. The Quick Terrain Modeler builds point clouds by placing the points exactly where they belong in 3-D space. There is no interpolation or approximation. It is a good way to visualize the extents of a survey, the data density (where point coverage is “thick” or “thin”), survey coverage (gaps between airborne survey strips will be exposed), data fidelity and data anomalies. Point clouds display the detail of non-massive objects (e.g., trees, bridges, power lines, transmission line poles, microwave towers, etc.) better than a surface model. Surface Models (.qst) are good for visualizing terrain and creating “gridded” data sets. The Quick Terrain Modeler builds a surface model by laying out a regular grid across the survey area and placing a height value on all of the vertices. It then builds a solid surface across this grid. The process involves an approximation of data values. Since the result is a solid surface, the effect is more visually realistic. Surface models are very good for spotting patterns in a terrain (e.g., for archaeology – looking for ruins that may be only a few centimeters high in a vast area), analyzing changes to a large area, and creating realistic presentations and “fly-throughs.”

The surface model represents the bare-earth and the object model represents the foliage above surface up to a certain height (inserted during bare-earth plug-in procedure and the cloud model classification represents the foliage that exists above object files).

Some additional parameters allow the users to enter values that affect the classification data.

(a) *Minimum Resolution, Maximum Surface Slope, Maximum Surface Delta* which determines whether points should be part of the surface or not, *Maximum Surface Variation* which by default is 0.1 m, but in foliage areas, the value should be reduced to increase the discrimination.

(b) Import Model on Completion Panel includes some import options such as:
i) *color code models by classification*. When this button is selected, then discrete colors are assigned in each classification model.

surface – blue

cloud – green

object - red

ii) *import surface file as surface model*. This parameter will be used to define the underlying grid spacing for the model. This specified value should be set to correspond to the density of the original data set.

iii) *import AGL into Alpha channel*. This button imports AGL information and can later be used for QTM alpha filtering capability to clip points above or below a specific height.

iv) *AGL Upper limit*. This value is used to classify points as cloud or object. Points above upper limits will be classified as clouds and points below will be classified as objects.

(c) The last and very important step is to select the ASCII format and the proper Geo-Registration parameters to provide all the information that the process must properly read and load the input XYZ file.

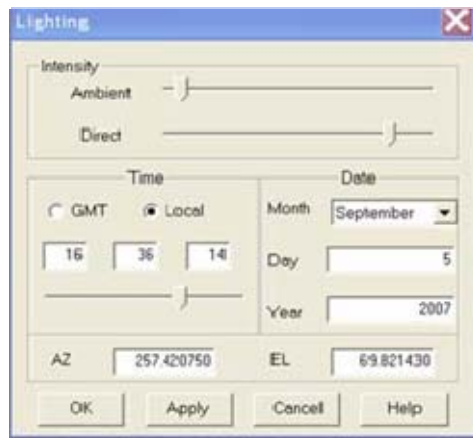
B. DISPLAY TOOLS

After the bare extraction process, the created surface and object models were loaded to identify possible trails and roads. Although one area was identified as a trail, other trails were not visible in the data analysis. More trails were clearly identified in the data upon further evaluation of the data and terrain features analysis. It is difficult to distinguish between waterways or drainage areas and trails or walking paths. The incorrect trail identification appeared to be a dry river or creek with extremely dense vegetation.

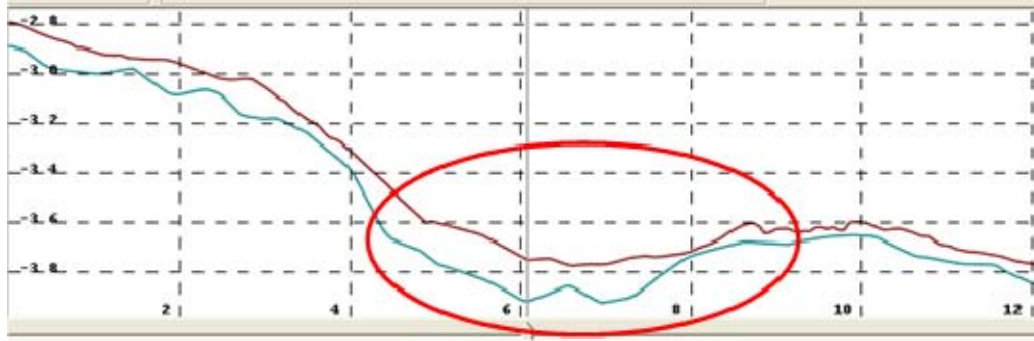
Some tools within Quick Terrain Modeler were used to extract more trails and roads correctly. The *Toggle Vertex Colors* button turns on/off any colors embedded in the models to eliminate the dark areas in the LIDAR images, due to shadow effects, and intensity or RGB profile imported with the model. However, trails are identified as dark lines, so it needs to be off. Also, the *Toggle Height Coloration* button turns height coloration on and off.

The *Configure Height Coloration* button allows the user to alter the height palette or the height mapping by pressing the Configure Height Coloration button or by selecting Configure Height Coloration from the Textures menu. This will summon a dialog window with sliders representing the minimum and maximum Z over which to spread the colors. With this toggle, the terrain scale models were modified by different colors based on the terrain morphology. It makes it easier to differentiate between the terrain depressions of the trails.

One of the most important buttons is the *Set Lighting* tool, which is useful for manipulating the lighting to achieve maximum relief in the model or to brighten the model. This setting makes it possible to manipulate model lighting in two ways. First, it is possible to directly control the intensity of the ambient and direct lighting and second, to also set the current lighting angle and appropriate time and date.



The most useful tool found on the display buttons was the *Place Mensuration Line*. By drawing a line across a trail, many characteristics can be determined like the width and the topography profile of the selected points in the interested area. It offers the ability to configure the location of a trail, whether it is under or above the slope. Using the same tool, trail or road measurement can be done for planning purposes. Pop-up boxes under this button's control provide the length of the placing line along the trail and give the direction from starting to ending point.



Show/Hide Models displays or hides open models. This is a very useful tool for isolating individual models without closing them. Users must click on the individual model names to display or hide each individual model. Users can press the “Show All” button to display quickly all models simultaneously, “Hide All” to start with no models loaded, or “Invert All” to toggle quickly between the visible and hidden models. Note: When a subset of loaded models is visible, resetting the view (from the primary button bar) will only reset the view to the extent of the visible model(s), rather than to the extent of all.

THIS PAGE INTENTIONALLY LEFT BLANK

APPENDIX B. ACCURACY TEMPLATES

Sequoia National Park

Sub-Area 1

Sequoia National Park		
Sub-Area 1		
Points		
Target Points	Measured distance from point (Real-Absolute values) (m)	
1	0.40	0.40
2	-0.30	0.30
3	0.50	0.50
4	-0.20	0.20
5	-0.50	0.50
6	0.90	0.90
7	-0.70	0.70
8	-0.50	0.50
9	-0.20	0.20
10	0.30	0.30
11	0.50	0.50
12	0.90	0.90
13	-0.40	0.40
14	0.60	0.60
15	-0.20	0.20
16	-0.70	0.70
17	-0.40	0.40
18	0.30	0.30
19	0.50	0.50
20	0.20	0.20
21	-0.20	0.20
22	0.10	0.10
23	0.20	0.20
24	0.40	0.40
25	-0.50	0.50
26	0.20	0.20
27	0.40	0.40
28	0.90	0.90
29	-0.10	0.10
30	-0.20	0.20
31	-0.50	0.50
32	0.20	0.20
Mean of the real values (m)	0.06	
Mean of the absolute values (m)	0.41	
RMS (m)	0.466703868	
Average of points inside the trail	26 of 32 = 81.25 %	

Sequoia National Park	
Sub-Area 1	
Points	
Control Points	Measured distance from point (Real-Absolute values) (m)
1	0.40
2	0.30
3	0.50
4	0.10
5	0.10
6	0.20
7	0.30
8	0.40
9	0.60
10	0.40
11	0.50
12	0.70
13	0.50
14	0.20
15	0.10
16	0.60
17	0.50
18	0.20
19	0.10
Mean of the absolute values (m)	0.35
RMS (m)	0.399341563
Average of points inside the trail	16 of 19 = 84.21 %

Sub-Area 2

Sequoia National Park		
Sub-Area 2		
Points		
Target Points	Measured distance from point (Real-Absolute values) (m)	
1	0.30	0.30
2	0.20	0.20
3	-0.40	0.40
4	-0.10	0.10
5	0.50	0.50
6	-0.20	0.20
7	-0.30	0.30
8	0.30	0.30
9	0.20	0.20
10	0.20	0.20
11	-0.50	0.50
12	-0.70	0.70
13	0.30	0.30
14	0.20	0.20
15	-0.80	0.80
16	0.90	0.90
17	-0.40	0.40
18	-0.30	0.30
19	-0.20	0.20
20	-0.50	0.50
21	-0.20	0.20
22	0.30	0.30
Mean of the real values (m)	-0.05	
Mean of the absolute values (m)		0.36
RMS (m)	0.417786374	
Average of points inside the trail	19 of 22 = 86.36 %	

Sequoia National Park	
Sub-Area 2	
Points	
Control Points	Measured distance from point (Real-Absolute values) (m)
1	0.10
2	0.20
3	0.70
4	0.40
5	0.20
6	0.10
7	0.30
8	0.50
9	0.40
10	0.40
11	0.50
12	0.20
13	0.50
14	0.20
15	0.40
16	0.50
17	0.30
Mean of the absolute values (m)	0.35
RMS (m)	0.382714761
Average of points inside the trail	16 of 17 = 94.12 %

Sub-Area 3

Sequoia National Park		
Sub-Area 3		
Points		
Target Points	Measured distance from point (Real-Absolute values) (m)	
1	1.20	1.20
2	0.70	0.70
3	0.40	0.40
4	0.50	0.50
5	0.50	0.50
6	-0.10	0.10
7	0.40	0.40
8	-0.20	0.20
9	-0.10	0.10
10	0.30	0.30
11	-0.40	0.40
12	-0.10	0.10
Mean of the real values (m)	0.26	
Mean of the absolute values (m)		0.41
RMS (m)	0.505799697	
Average of points inside the trail	10 of 12 = 83.33 %	

Sequoia National Park		
Sub-Area 3		
Points		
Control Points	Measured distance from point (Real-Absolute values) (m)	
1		0.60
2		0.50
3		0.30
4		0.40
5		0.50
6		0.50
7		0.20
8		0.50
9		0.70
10		0.20
11		0.40
Mean of the absolute values (m)	0.44	
RMS (m)	0.461223669	
Average of points inside the trail	9 of 11 = 81.81 %	

Points and Sizes

Sequoia National Park

SEQUOIA POINTS AND SIZES				
Type Areas	Target Size(m ²)	Target points	Control (m ²)	Control points
Sub Area-1	1922	32	1900	19
Sub Area-2	5990	22	6000	17
Sub Area-3	2102	12	2100	11

Fort Belvoir

FORT BELVOIR POINTS AND SIZES				
Type Areas	Target Size(m ²)	Target Points	Control Size (m ²)	Control Points
Sub Area-1A_1	731	11	740	7
Sub Area-1A_2	410	8	410	5
Sub Area-1A_3	2688	34	2700	26
Sub Area-1A_4	838	12	840	8
Sub Area-1A_30	596	8	600	5
Sub Area-1A_31	541	15	540	10
Sub Area-1A_32	446	20	450	16
Sub Area-2_2	10714	60	10720	40

TOTAL RESULTS

Sequoia National Park									
LIDAR vs. MANUAL									
Target points						Control points			
AREAS	Total Numbers	Mean of the real values (m)	Mean of the absolute values (m)	RMS (m)	Average of points inside the trail	Total Numbers	Mean of the absolute values (m)	RMS (m)	Average of points inside the trail
Sub-Area 1	32	0.06	0.41	0.467	81,25%	19	0.35	0.399	82,21%
Sub-Area 2	22	-0.05	0.36	0.418	86,36%	17	0.35	0.383	94,12%
Sub-Area 3	12	0.26	0.41	0.506	83,33%	11	0.44	0.461	81,81%
TOTAL	66					47			
AVERAGE		0.090	0.393	0.463	0.836		0.380	0.414	0.860

LIST OF REFERENCES

- Abbot, R. H., Lane, D. W., Sinclair, M. J., & Spruing, T. A. (1996). Lasers chart the waters of Australia's Great Barrier Reef. *Proc. SPIE*, 2964, 72-90.
- Ahokas, E. et al. (2003). A quality assessment of airborne laser scanner data. *The International Archives of the Photogrammetry, Remote Sensing and Spatial Information Sciences*, Dresden, Germany, XXXIV-3/W13.
- Airborne and Spaceborne Lasers. (1999, November 9-11). *ISPRS WG III/5: Remote Sensing and Vision Theories for Automatic Scene Interpretation; ISPRS WG III/2: Algorithms for Surface Reconstruction; International Archives of Photogrammetry and Remote Sensing*; XXXII-3/W14, La Jolla, CA. Retrieved November 22, 2008, from <http://www.isprs.org/commission3/lajolla/>
- Airborne Laser Mapping. A reference source on an emerging technology: The skinny. Retrieved June 26, 2008, from <http://www.airbornelasermapping.com/ALMSkinny.html>
- Airborne1. (2008). LIDAR accuracy booklet. Retrieved October 26, 2008, from http://www.airborne1.com/technology/Statement_of_Accuracy_and_Deliverables.pdf
- Amar, Nayegandhi. (2006). LIDAR technology overview. Presented at the ETI –US Geological Survey. Retrieved August 17, 2008, from http://LIDARLIDAR.cr.usgs.gov/downloadfile2.php?file=Nayegandhi_LIDAR_Technology_Overview.pdf
- Bartels, M., & Wei, H. (2007, August 15). Remote sensing: Segmentation and classification of LIDAR data. Retrieved November 12, 2008, from <http://www.cvg.rdg.ac.uk/projects/LIDAR/index.html>
- Brandtberg, T., Warner, T. A., Landenberger, R. E., & McGraw, J. B. (2003). Detection and analysis of individual leaf-off tree crowns in small footprint, high sampling density LIDAR data from the eastern deciduous forest in North America. *Remote Sensing of Environment*, 85, 290.
- Caldwell, Jason. (March/April 2005). Merging technologies - LIDAR complements multispectral imagery. *Earth Imaging Journal*.
- Chauve, A., Mallet C., Bretar F., Durrieu S., Deseilligny Marc P., & Puech W. (2007, September 12-14). Processing full-waveform LIDAR data: Modelling raw signals. *ISPRS Workshop on Laser Scanning 2007 and SilviLaser 2007*, Finland. Retrieved October 14, 2008, from http://www.commission3.isprs.org/laser07/final_papers/Chauve_2007.pdf

- Dubayah, R., Blair, J. B., Bufton, J. L., Clark, D. B., JaJa, J., Knox, R., Luthcke, S. B., Prince, S., & Weishampel, J. The vegetation canopy LIDAR mission, *Proceedings of Land Satellite Information in the Next Decade, II: Sources and Applications*. Bethesda, MD: American Society of Photogrammetry and Remote Sensing, 100-112.
- Ducic, V., Hollaus, M., Ullrich A., Wagner W., & Melzer T. (2006, February 14-15). 3-D vegetation mapping and classification using full-waveform laser scanning. Presented at the Workshop on 3-D Remote Sensing in Forestry, Vienna– Session 8a, Retrieved October 14, 2008, from http://www.ipf.tuwien.ac.at/publications/vd_mh_ww_tm_2006_3-D_Forestry_Remote_Sensing.pdf
- Emison, Bill. (2008, February 22). Request for proposal (RFP) development for LIDAR data collection projects. Paper presented at the International LIDAR Mapping Forum, Denver, CO.
- Ensminger, Chris. (2007). IowaDNR interactive mapping. *The Iowa Department of Natural Resources*. Retrieved September 19, 2008, from <http://www.iowadnr.com/mapping/LIDAR/faq.html>
- Espinoza, F., & Owens, E. R. Identifying roads and trails hidden under canopy using LIDAR. (2007). Master's Thesis, Naval Postgraduate School.
- Forestry Commission. *Forestry Commission Great Britain*. Retrieved September 26, 2008, from <http://www.forestry.gov.uk/>
- Forsberg, R., Hvidegard, S. M., & Keller, K. (2003). Airborne LIDAR measurement of sea-ice thickness. Geophysical Research Abstracts. *European Geophysical Society*, 5, 09612.
- Fort Belvoir. (2008). *Official site of Fort Belvoir, Virginia*. Retrieved August 18, 2008, from <http://www.belvoir.army.mil/>
- Foxgrover, Amy C., & Jaffe, Bruce E. (2005). South San Francisco Bay 2004 topographic LIDAR survey: Data overview and preliminary quality assessment. *USGS*, 8-9.
- Garwin, Laura, & Lincoln, Tim. (2003). The first laser. *A Century of Nature: Twenty-One Discoveries that Changed Science and the World*, 107-12.
- Geusic, J. E., Marcos, H. M., & Van Uitert, L. G. (1964). Laser oscillations in Nd-doped yttrium aluminum, yttrium gallium and gadolinium garnets. *Applied Physics Letters*, 4(10), 182-184.

- Global Security Organization. Airborne measure countermeasures: Rapid Airborne Mine Clearance System (RAMICS). Retrieved July 5, 2008, from <http://www.globalsecurity.org/military/library/budget/fy2001/dote/navy/01amc.html>
- Global Security Organization. Military extract of STANAG 2174 (Edition 4): Military routes and route/road networks. Retrieved October 19, 2008, from <http://www.globalsecurity.org/military/library/policy/army/fm/55-30/appc.htm>
- Guenther, G. C., & Mesick, H. C. (1988). Analysis of airborne laser hydrography waveforms. *Proceedings SPIE Ocean Optics IX*, 925, 232-241.
- Hofton, M. A., Rocchio, L. E., Blair, J.B., & Dubayah, R. (2002). Validation of vegetation canopy Lidar sub-canopy topography measurements for a dense tropical forest. *Journal of Geodynamics*, 34, 491-502.
- Hug, C., Ullrich, A., & Grimm, A. (2004, October 3 – October 6). LiteMapper 5600. A waveform-digitizing LIDAR terrain and vegetation mapping system. NatScan Conference 2004, Freiburg, Germany. Laser-scanners for forest and landscape assessment - instruments, processing methods and applications. Freiburg im Breisgau, German; *International Archives of Photogrammetry, Remote Sensing and Spatial Information Sciences*, XXXVI, Part 8/W2.
- Kalogirou, V. (2006, September). Simulation of discrete-return LiDAR signal from conifer stands for forestry applications. MSc Thesis, University of London MSc in Remote Sensing, University College London.
- Kenyon, Henry S. (2002). LIDAR illuminates optical sensors. Retrieved July 23, 2008, from http://www.afcea.org/signal/articles/templates/SIGNAL_Article_Template.asp?articleid=367&zoneid=64
- Krabill, W. B., Collins, J. G., Link, L. E., Swift, R. N., & Butler, M. L. (1984). Airborne laser topographic mapping results; photogrammetric engineering & remote sensing, 50, 685-694.
- Laser Stars. *Lasestars.org*. Retrieved December 1, 2008, from <http://lasestars.org/history/ruby.html>
- Lefsky, A. Michael, Harding, J. David, Keller, Michael, Warren, Cohen B., Carabajal, C., Claudia, Fernando del Bom Espirito-Santo, Hunter, O. Maria, & Raimundo, de Oliveira Jr. (2005). Estimates of forest canopy height and aboveground biomass using ICESat. *Geophysical Research*, 32, L22S02.
- Lefsky, Michael A., Cohen, Warren B., Parker, Geoffrey G., & Harding, David J. (2002, January 1). LIDAR remote sensing for ecosystem studies. *BioScience*.

- Lewis, P., & Hancock, S. (2007, January 23). LIDAR for vegetation applications. UCL Department of Geography, Gower St, London, UK. Retrieved September 2, 2008, from www.geog.ucl.ac.uk/~plewis/lidarforvegetation/LiDARforVegetationApplications.doc
- LIDARcomm. Second largest forest products company realizes multiple benefits from LIDAR and ortho imagery. Retrieved August 21, 2008, from <http://LIDARcomm.com/id23.html>
- Maiman, T. H. (1960, August 6). Stimulated optical radiation in ruby. *Nature*, 187, 493.
- Mangold, Roland. (2008, February 1). Points of light. A discussion about the LIDAR production process. Retrieved September 2, 2008, from http://www.pobonline.com/Articles/Article_Rotation/BNP_GUID_9-5-2006_A_1000000000000242390
- Means, J. E., Acker, S. A., Harding, D. J., Blair, J. B., Lefsky, M. A., Cohen, W. B., Harmon, M. E., & McKee, W. A. (1999, March). Use of large-footprint scanning airborne LIDAR to estimate forest stand characteristics in the western cascades of Oregon - biomass distribution and production budgets. *Remote Sensing of Environment*, 67(3), 298-308(11).
- NASA. Goddard space flight center – laser vegetation imaging sensor. *About LVIS*. Retrieved September 7, 2008, from https://lvis.gsfc.nasa.gov/index.php?option=com_content&task=blogcategory&id=96&Itemid=93
- National Park Service. (2004). U.S. Department of the Interior – Interagency trail data standards. *Trail Planning and Management Fundamentals*. Retrieved October 14, 2008, from <http://www.nps.gov/gis/trails/documents/AppendixA.doc>
- Optech. *Optech incorporated*. Retrieved September 29, 2008, from <http://www.optech.ca/index.htm>
- Prasad, Hanuman C. Experiences on digital photogrammetry and remote sensing - A production perspective. Paper presented for Infotech Enterprises Ltd. at the Map World Forum in Hyderabad, India.
- Rowe, Aaron. (2007, June 19). Mapping a redwood forest with LIDAR. *Wired Science-Environment*. Retrieved August 27, 2008, from http://blog.wired.com/wiredscience/2007/06/mapping_a_redwo.html
- Schawlow, A. L., & Townes, C. H. (1958). Infrared and optical masers. *Phys. Rev.* 112(6), 1940.

- Schlagintweit, G. (1995). Discussion of (RoxAnn) operations. Remote sensing techniques for subtidal classification, workshop. Institute of Ocean Sciences, Sydney, B.C., 5-7.
- SIMoN. Sanctuary Integrated Monitoring Network. Retrieved July 18, 2008, from <http://www.sanctuariesimon.org>
- Solodukhin, V .I., Zukov, A. Ya, & Mazugin, I. N. (1977). Possibilities of laser aerial photography for forest profiling. *Lesnoe Khozyaistvo (Forest Management)*, 10, 53-58, (in Russian).
- TopoSys. *Topographic system*. Retrieved November 12, 2008, from <http://www.toposys.com/toposys-en/LIDARLIDAR-systems/airborne-laserscanning.php?print=true>
- Uddin, W., & E. Al-Turk. (2001, August 11-14). Airborne LIDAR digital terrain mapping for transportation infrastructure asset management. *Proceedings, Fifth International Conference on Managing Pavements*, Seattle, Washington.
- UIDAHO. University of Idaho. College of Natural Resources. Retrieved October 14, 2008, from <http://www.cnrhome.uidaho.edu>
- USGS. U.S. Geological Survey Earth Science Information Sources. Retrieved October 19, 2008, from www.soundwaves.usgs.gov/2007/09/meetings2.html
- Valtus. Valtus Imagery Services. Retrieved October 14, 2008, from <http://www.valtus.com>
- White, Mike. (2003, June). *Sequoia National Park: A Complete Hikers Guide*, 28-25.
- Zwally, H., Schutz, B., Abdalati, W., Abshire, J., Bentley, C., Brenner, A., Bufton, J., Dezio, J., Hancock, D., Harding, D., Herring, T., Minster, B., Quinn, K., Palm, S., Spinhirne, J., & Thomas, R. (2002). ICESat's laser measurements of polar ice, atmosphere, ocean, and land. *Journal of Geodynamics*, 34(3), 405-445.

THIS PAGE INTENTIONALLY LEFT BLANK

INITIAL DISTRIBUTION LIST

1. Defense Technical Information Center
Ft. Belvoir, Virginia
2. Dudley Knox Library
Naval Postgraduate School
Monterey, California
3. R.C. Olsen
Naval Postgraduate School
Monterey, California
4. David C. Jenn
Naval Postgraduate School
Monterey, California
5. Michael Roth
Johns Hopkins University Applied Physics Lab
Laurel, Maryland
6. Embassy of Greece,
Office of Naval Attaché
Washington, D.C.
7. Embassy of Greece,
Office of Air Attaché
Washington, D.C.
8. Apostolos Karatolios
Larissa, Greece
9. Prokopios Krougios
Korydallos, Greece